

Structure-Preserving Reduced Basis Methods for Poisson Systems

Jan S. Hesthaven* and Cecilia Pagliantini†

Abstract

We develop structure-preserving reduced basis methods for a large class of nondissipative problems by resorting to their formulation as Hamiltonian dynamical systems. With this perspective, the phase space is naturally endowed with a Poisson manifold structure which encodes the physical properties, symmetries, and conservation laws of the dynamics. The goal is to design reduced basis methods for the general state-dependent degenerate Poisson structure based on a two-step approach. First, via a local approximation of the Poisson tensor, we split the Hamiltonian dynamics into an “almost symplectic” part and the trivial evolution of the Casimir invariants. Second, canonically symplectic reduced basis techniques are applied to the nontrivial component of the dynamics, preserving the local Poisson tensor kernel exactly. The global Poisson structure and the conservation properties of the phase flow are retained by the reduced model in the constant-valued case and up to errors in the Poisson tensor approximation in the state-dependent case. A priori error estimates for the solution of the reduced system are established. A set of numerical simulations is presented to corroborate the theoretical findings.

Keywords. Hamiltonian dynamics, Poisson manifolds, symplectic structure, invariants of motion, structure-preserving schemes, reduced basis methods (RBM).

MSC 2010. 15A21, 53D17, 53D22, 37N30, 37J35, 78M34, 65P10

1 Introduction

During the last decade there has been substantial developments of model order reduction techniques to efficiently solve parameterized differential equations in computationally intensive scenarios such as real-time and many-query problems. Reduced basis methods (RBM) aim at reducing the computational effort by replacing the original high-dimensional problems with models of significantly reduced dimensionality without compromising the overall accuracy. For time-dependent parametric problems, an approximation space of low dimension, the so-called *reduced space*, is constructed from a collection of full-order solutions at sampled values of time and parameters during a computationally intensive offline phase. The reduced space is spanned by the modes associated with the “dominant” components of the dynamics. In the online phase the reduced order model is then solved at a substantially reduced computational cost for any parameter.

The development of reduced basis techniques for the efficient solution of differential equations is well-established in the context of linear elliptic PDEs and dissipative systems. For time-dependent nondissipative problems, which can often be modeled as a Hamiltonian system, model order reduction is less well understood. Indeed, stability becomes a major concern in this context as the stability properties of the high-fidelity problem are not generally inherited by the reduced model, even when a very accurate reduced space is used. Moreover, the phase space of Hamiltonian dynamics is endowed with

*Computational Mathematics and Simulation Science (MCSS), EPFL-SB-MATH-MCSS, École Polytechnique Fédérale de Lausanne (EPFL), CH-1015 Lausanne, Switzerland. Email: jan.hesthaven@epfl.ch

†*Corresponding author.* Centre for Analysis, Scientific computing and Applications, Department of Mathematics and Computer Science, Eindhoven University of Technology (TU/e), 5600 MB Eindhoven, The Netherlands. Email: c.pagliantini@tue.nl

a differentiable Poisson manifold structure that underpins the physical properties of the system, such as symmetries, families of conserved quantities, and invariants. In the most general case, the Poisson structure is *state-dependent*, i.e. it changes over the phase space, and it is not full rank. This geometric structure of the phase flow is in general destroyed during model order reduction, resulting in spurious and unphysical artifacts which may trigger instabilities and generate qualitatively wrong solutions.

The literature on model order reduction for hyperbolic and conservative equations has recently seen the development of methods which aim at preserving the geometric structure of dynamical systems. In the context of nondissipative Hamiltonian problems Lall et al. [30] pioneered the use of a Galerkin projection on the Euler–Lagrange equations to devise reduced order models which preserve Lagrangian structures. A similar approach was pursued and improved in [12]. Dealing directly with the Hamiltonian formulation, reduced basis methods preserving the *canonical* symplectic structure of dynamical systems has been developed in [40] and [2].

To the best of our knowledge, none of the aforementioned works address the general case of degenerate and/or state-dependent Poisson structures. A naïve extension of the available reduction techniques to these cases is not possible as an orthogonal or symplectic projection of the full Hamiltonian model onto the reduced space does not guarantee that the reduced flow is Hamiltonian with a Poisson phase space, nor that the degeneracy of the structure is retained by the reduced model.

Our Contribution: Novelty and Outline. We consider parameterized finite-dimensional Hamiltonian dynamical systems of the form

$$\begin{cases} \partial_t u(t, \eta) = \mathcal{J}_N(u) \, \mathrm{d}\mathcal{H}_N, & \text{for } t > t_0, \\ u(t_0, \eta) = u_0(\eta). \end{cases} \quad (1.1)$$

Here the unknown u depends on time and on a set of parameters $\eta \in \Lambda$ where $\Lambda \subset \mathbb{R}^d$ is compact, with $d \geq 1$, d denotes the exterior derivative, \mathcal{H}_N is the Hamiltonian function, and $\mathcal{J}_N(u)$ is a finite-dimensional operator encoding the Poisson manifold structure.

Many relevant models in mathematical physics can be written as Hamiltonian systems: to name a few, in classical mechanics, the rigid body motion and related n -body problem, the harmonic oscillator, the dynamical billiard, the Euler top equations, the Hénon–Heiles problem; in quantum dynamics, the Heisenberg equation, the May–Leonard model and the Maxwell–Bloch equations; in population and epidemics dynamics, certain Lotka–Volterra models or the Kermack–McKendrick equations, etc..

The evolution equation (1.1) can also be thought of as the semi-discrete formulation ensuing from the numerical approximation of partial differential equations that can be derived from action principles. Examples of such problems include Maxwell’s equations, Schrödinger’s equation, Korteweg–de Vries and the wave equation, compressible and incompressible Euler equations, Vlasov–Poisson and Vlasov–Maxwell equations. Observe that, when dealing with Hamiltonian PDEs, we require a spatial discretization of the aforementioned problems that is structure-preserving, in the sense of yielding a semi-discrete system of the form (1.1). Although systematic approaches to discretize Hamiltonian PDEs with general Poisson structures are still largely unavailable, this is a very active research area that has recently seen several successful results like the GEMPIC method for plasma models [29], the finite element method proposed in [38] for incompressible Euler equations in the Arnold formulation [3] and the Energy-Momentum-Entropy method for finite strain thermoelastodynamics [8].

The relevance of nondissipative problems of the form (1.1) and the lack of reduced models that are able to preserve the intrinsic structure of general Hamiltonian dynamics motivate this work. We propose a novel reduced basis method for general parameterized Hamiltonian problems that ensures that the reduced dynamics retain the Poisson structure of the local phase flow. Our method is based on two steps. In the first step we perform locally, in each point of the phase space, a splitting of the Hamiltonian dynamics into a canonically symplectic component and a trivial evolution of the invariants associated with the kernel of the Poisson structure. The splitting of the dynamics is motivated by a result of Darboux [20] which, roughly speaking, demonstrates the existence of local charts in which any Poisson structure has the canonical form. The rationale is that canonical Poisson structures are more amenable to model order reduction since the nonlinearity has been removed from the structure and its kernel singled out. A major issue in this step is that an analytic expression of the Darboux charts is in most cases unavailable.

Hence, standard approximations of the structure, even if local, are prone to destroy the Hamiltonian nature of the dynamics. Failing to preserve the Poisson structure of the phase space, even by a small error, may propagate uncontrollable instabilities along the dynamics and compromise the stability and accuracy of the solution. To address this problem, we propose local approximations of the Darboux charts by leveraging the linearization introduced by the timestepping. The “freezing” of the Poisson structure at each stage of the temporal integration allows us to locally rewrite the original Hamiltonian dynamics into canonical form. After having characterized the approximability properties of the split dynamics, we perform a second step in which the canonical Hamiltonian dynamics is approximated in a lower-dimensional manifold foliated by the Poisson tensor kernel and a reduced symplectic component. For the latter we construct a symplectic reduced basis via algorithms adapted from [40, 2].

A theoretical foundation of the proposed method is presented: we derive convergence results for the reduced basis algorithm, characterize the properties of the reduced dynamics in terms of invariants and Lyapunov stability, and establish a priori error estimates with respect to the full model solution. We show that the reduced dynamics resulting from our approach retains the Poisson structure of the phase flow up to the local approximation error of the Darboux charts.

The remainder of the paper is organized as follows. In Section 2, the algebraic structure underlying Hamiltonian systems on finite-dimensional Poisson manifolds is described. Section 3 pertains to degenerate constant-valued parametric Poisson structures and provides preparatory results for the more challenging case of state-dependent structures. In this simpler case, the manifold splitting is performed *globally*. We show in Section 3.2.1 that the resulting reduced problem is Hamiltonian with a Poisson manifold structure and inherits the physical properties of the high-fidelity model in terms of conservation of the Hamiltonian, preservation of the Casimir invariants, and Lyapunov stability. In Section 3.3 the structure-preserving reduced basis method is coupled to a symplectic DEIM for the efficient treatment of the nonlinear terms. State space error bounds for the solution of the reduced system are established in terms of the projection error into the reduced space. Next, Section 4 is devoted to the case of state-dependent Poisson structures. In Section 4.1 we introduce the Poisson maps which locally approximate the Darboux change of coordinates and recast the local discrete dynamics into the split form. The structure-preserving properties of the resulting reduced dynamics are discussed in Section 4.2. A priori error estimates for the fully discrete reduced problem are established in Section 4.3. In Section 5 a set of numerical experiments is presented and conclusions are drawn in Section 6.

2 Dynamical Systems with Poisson Structure

In this Section we briefly describe the topological and algebraic structure underlying the phase space of Hamiltonian dynamical systems (1.1), where, for the sake of better readability, we omit the explicit dependency on the parameter η .

Definition 2.1 (Poisson Structure). Let \mathcal{V}_N be a finite N -dimensional smooth manifold. A *Poisson structure* on \mathcal{V}_N is a bilinear operation $\{\cdot, \cdot\}_N : C^\infty(\mathcal{V}_N) \times C^\infty(\mathcal{V}_N) \rightarrow C^\infty(\mathcal{V}_N)$, called a *bracket*, with the following properties: for all $\mathcal{F}, \mathcal{G}, \mathcal{I} \in C^\infty(\mathcal{V}_N)$ and $u \in \mathcal{V}_N$,

- (i) Skew-symmetry: $\{\mathcal{F}, \mathcal{G}\}_N(u) = -\{\mathcal{G}, \mathcal{F}\}_N(u)$.
- (ii) Leibniz rule: $\{\mathcal{F}\mathcal{G}, \mathcal{I}\}_N(u) = \{\mathcal{F}, \mathcal{I}\}_N(u)\mathcal{G}(u) + \mathcal{F}(u)\{\mathcal{G}, \mathcal{I}\}_N(u)$.
- (iii) Jacobi identity: $\{\mathcal{F}, \{\mathcal{G}, \mathcal{I}\}_N\}_N(u) + \{\mathcal{G}, \{\mathcal{I}, \mathcal{F}\}_N\}_N(u) + \{\mathcal{I}, \{\mathcal{F}, \mathcal{G}\}_N\}_N(u) = 0$.

A manifold endowed with a Poisson structure is called a *Poisson manifold*.

The space $C^\infty(\mathcal{V}_N)$ of real-valued smooth functions over the Poisson manifold $(\mathcal{V}_N, \{\cdot, \cdot\}_N)$ together with the bracket $\{\cdot, \cdot\}_N$ forms a Lie algebra [1, Proposition 3.3.17], called the *Poisson algebra* of \mathcal{V}_N .

By the bilinearity of $\{\cdot, \cdot\}_N$ and the Leibniz rule, given an analytic function $\mathcal{H} \in C^\infty(\mathcal{V}_N)$, the map $\mathcal{F} \in C^\infty(\mathcal{V}_N) \mapsto \{\mathcal{F}, \mathcal{H}\}_N \in C^\infty(\mathcal{V}_N)$ defines differentiation on the Poisson manifold \mathcal{V}_N . Hence, there exists a locally *unique* vector field $X_{\mathcal{H}}(u)$ belonging to $T_u\mathcal{V}_N$, the tangent space at \mathcal{V}_N in u , such that $\mathbf{L}_{X_{\mathcal{H}}}\mathcal{F} = \{\mathcal{F}, \mathcal{H}\}_N$, where \mathbf{L}_X denotes the Lie derivative with respect to the velocity field X . The vector $X_{\mathcal{H}}(u)$ is called the *Hamiltonian vector field* of the function $\mathcal{H} \in C^\infty(\mathcal{V}_N)$, and characterizes the dynamics

of the evolution problem (1.1), as explained in Section 2.1. The map $\mathcal{H} \in C^\infty(\mathcal{V}_N) \mapsto X_{\mathcal{H}} \in T\mathcal{V}_N$ is a (anti)homomorphism between Lie algebras [34, Proposition 10.2.2].

If $d\mathcal{H}$ is the 1-form, defined by the exterior derivative of the function $\mathcal{H} \in C^\infty(\mathcal{V}_N)$, its Hamiltonian vector field $X_{\mathcal{H}}$ can be obtained as the image of $d\mathcal{H}$ under the vector bundle morphism $\mathcal{J}_N(u)$ defined, for any $u \in \mathcal{V}_N$, as

$$\begin{aligned} \mathcal{J}_N(u) : T^*\mathcal{V}_N &\longrightarrow T\mathcal{V}_N \\ d\mathcal{H} &\longmapsto X_{\mathcal{H}}(u) := \mathcal{J}_N(u)d\mathcal{H}. \end{aligned} \quad (2.1)$$

The Poisson bracket $\{\cdot, \cdot\}_N$ on \mathcal{V}_N can be expressed in terms of \mathcal{J}_N as

$$\{\mathcal{F}, \mathcal{G}\}_N(u) = {}_{T^*\mathcal{V}_N}\langle d\mathcal{F}, \mathcal{J}_N(u) d\mathcal{G} \rangle_{T\mathcal{V}_N}, \quad \forall \mathcal{F}, \mathcal{G} \in C^\infty(\mathcal{V}_N), \forall u \in \mathcal{V}_N, \quad (2.2)$$

where ${}_{T^*\mathcal{V}_N}\langle \cdot, \cdot \rangle_{T\mathcal{V}_N}$ denotes the duality pairing between the cotangent and the tangent bundle. The map \mathcal{J}_N is a contravariant 2-tensor on the manifold \mathcal{V}_N , commonly referred to as the *Poisson tensor*. The tensor \mathcal{J}_N is skew-symmetric with respect to the metric g on \mathcal{V}_N defined as $g(\nabla\mathcal{F}, \cdot) := {}_{T^*\mathcal{V}_N}\langle d\mathcal{F}, \cdot \rangle_{T\mathcal{V}_N}$, and ∇ is the Riemannian gradient. Hence, in local coordinates, the Poisson bracket reads

$$\{\mathcal{F}, \mathcal{G}\}_N(u) = \nabla\mathcal{F}(u)^\top \mathcal{J}_N(u) \nabla\mathcal{G}(u), \quad \forall \mathcal{F}, \mathcal{G} \in C^\infty(\mathcal{V}_N), \forall u \in \mathcal{V}_N.$$

In view of the relationship between the bracket $\{\cdot, \cdot\}_N$ and the tensor \mathcal{J}_N , the Poisson manifold structure on \mathcal{V}_N can be equivalently characterized as follows.

Lemma 2.2. *Let \mathcal{V}_N be a finite N -dimensional smooth manifold and let \mathcal{J}_N be the vector bundle map defined in (2.1). Then the bracket (2.2) is a Poisson structure as per Definition 2.1, if and only if \mathcal{J}_N is skew-symmetric and satisfies the Jacobi identity*

$$\sum_{\ell=1}^N \left(\frac{\partial(\mathcal{J}_N(u))_{i,j}}{\partial u_\ell} (\mathcal{J}_N(u))_{\ell,k} + \frac{\partial(\mathcal{J}_N(u))_{j,k}}{\partial u_\ell} (\mathcal{J}_N(u))_{\ell,i} + \frac{\partial(\mathcal{J}_N(u))_{k,i}}{\partial u_\ell} (\mathcal{J}_N(u))_{\ell,j} \right) = 0, \quad (2.3)$$

for all $u \in \mathcal{V}_N$ and $i, j, k = 1, \dots, N$.

We say that the Poisson structure and the Poisson tensor are constant-valued if the morphism $\mathcal{J}_N(u)$ defined in (2.1) is independent of $u \in \mathcal{V}_N$. From (2.3), it immediately follows that any constant-valued skew-adjoint operator gives a Poisson structure.

In general, the vector bundle map (2.1) is not an isomorphism: its rank at a given point $u \in \mathcal{V}_N$ defines the *rank* of the Poisson manifold \mathcal{V}_N at u . By the skew-symmetry of the Poisson bracket, the rank of a Poisson manifold is always an even (non-negative) integer. Moreover, if \mathcal{V}_N is not full rank then its Poisson structure is said to be *degenerate*. Degeneracy of Poisson structures generates conservation laws of the Hamiltonian dynamics on the phase space \mathcal{V}_N , cf. Definition 2.6.

The notion of rank characterizes *symplectic* manifolds as those Poisson manifolds which have maximal global rank. Symplectic manifolds are endowed with a nondegenerate, closed 2-form ω , called a *symplectic structure*. The Poisson bracket on the symplectic manifold (\mathcal{V}_N, ω) is defined as

$$\{\mathcal{F}, \mathcal{G}\}_N(u) = \omega(X_{\mathcal{F}}, X_{\mathcal{G}}) := \omega(\mathcal{J}_N(u) d\mathcal{F}, \mathcal{J}_N(u) d\mathcal{G}), \quad \forall \mathcal{F}, \mathcal{G} \in C^\infty(\mathcal{V}_N), \forall u \in \mathcal{V}_N.$$

Since ω is nondegenerate, the map $\omega_{X_{\mathcal{H}}}^\flat : Y \in T\mathcal{V}_N \mapsto \omega(X_{\mathcal{H}}, Y) = (i_{X_{\mathcal{H}}}\omega)(Y)$ is injective (i_X denotes the contraction by X), and the Hamiltonian vector field $X_{\mathcal{H}}$ of the function $\mathcal{H} \in C^\infty(\mathcal{V}_N)$ satisfies $d\mathcal{H} = i_{X_{\mathcal{H}}}\omega$.

2.1 Hamiltonian Dynamics

The Hamiltonian vector field $X_{\mathcal{H}}$ characterizes the evolution problem (1.1), whose dynamics preserves the Poisson structure of the phase space.

Functions between Poisson manifolds, consistent with the structure in the sense of preserving the bracket, are called Poisson maps.

Definition 2.3 (Poisson Map). Let $(\mathcal{V}_N, \{\cdot, \cdot\}_N)$ and $(\mathcal{V}_n, \{\cdot, \cdot\}_n)$ be two Poisson manifolds of finite dimension N and n respectively, with $n \leq N$. A smooth map $\Psi : (\mathcal{V}_N, \{\cdot, \cdot\}_N) \rightarrow (\mathcal{V}_n, \{\cdot, \cdot\}_n)$ is called a *Poisson map* if

$$(\Psi^*\{\mathcal{F}, \mathcal{G}\}_n)(u) = \{\Psi^*\mathcal{F}, \Psi^*\mathcal{G}\}_N(u), \quad \forall \mathcal{F}, \mathcal{G} \in C^\infty(\mathcal{V}_n), \forall u \in \mathcal{V}_N.$$

A vector field $X_{\mathcal{H}}$ on a manifold \mathcal{V}_N determines a phase flow, namely a one-parameter group of diffeomorphisms $\Phi_{X_{\mathcal{H}}}^t : \mathcal{V}_N \rightarrow \mathcal{V}_N$ satisfying $d_t \Phi_{X_{\mathcal{H}}}^t(u) = X_{\mathcal{H}}(\Phi_{X_{\mathcal{H}}}^t(u))$ for all $t \in \mathcal{T}$ and $u \in \mathcal{V}_N$, with $\Phi_{X_{\mathcal{H}}}^0(u) = u$. The flow map $\Phi_{X_{\mathcal{H}}}^t$ of a vector field $X_{\mathcal{H}} \in T\mathcal{V}_N$ is Hamiltonian if $\Phi_{X_{\mathcal{H}}}^t$ is a Poisson map on its domain. The reverse is also true.

Proposition 2.4 ([34, Proposition 10.2.3]). *Let $(\mathcal{V}_N, \{\cdot, \cdot\}_N)$ be a Poisson manifold and $\mathcal{H} \in C^\infty(\mathcal{V}_N)$. Then, the map $\Phi_{X_{\mathcal{H}}}^t : \mathcal{V}_N \rightarrow \mathcal{V}_N$ satisfies*

$$\frac{d}{dt}(\mathcal{F} \circ \Phi_{X_{\mathcal{H}}}^t) = \{\mathcal{F}, \mathcal{H}\}_N \circ \Phi_{X_{\mathcal{H}}}^t, \quad \forall \mathcal{F} \in C^\infty(\mathcal{V}_N),$$

if and only if it is the flow of $X_{\mathcal{H}}$.

In addition to possessing a Poisson phase flow, Hamiltonian dynamics is characterized by the existence of differential invariants, and symmetry-related conservation laws.

Definition 2.5 (Invariants of Motion). A function $\mathcal{I} \in C^\infty(\mathcal{V}_N)$ is an *invariant of motion* of the dynamical system (1.1) with flow map $\Phi_{X_{\mathcal{H}_N}}^t$, and $X_{\mathcal{H}_N} := \mathcal{J}_N d\mathcal{H}_N$, if $\{\mathcal{I}, \mathcal{H}_N\}_N(u) = 0$ for all $u \in \mathcal{V}_N$. Consequently, \mathcal{I} is constant along the orbits of $X_{\mathcal{H}_N}$.

The Hamiltonian function (if time-independent) is an invariant of motion. A particular subset of the invariants of motion of a dynamical system is given by the *Casimir invariants*, i.e. functions on \mathcal{V}_N which $\{\cdot, \cdot\}_N$ -commute with every other function in $C^\infty(\mathcal{V}_N)$.

Definition 2.6 (Casimir Invariants). If \mathfrak{g} is a Lie algebra with Lie product $\{\cdot, \cdot\}$, the *centralizer* of a subset S of \mathfrak{g} is defined as $C_{\mathfrak{g}}(S) := \{\mathcal{C} \in \mathfrak{g} : \{\mathcal{C}, \mathcal{F}\} = 0 \text{ for all } \mathcal{F} \in S\}$. The centralizer $C_{\mathfrak{g}}(\mathfrak{g})$ of the Lie algebra itself is called the *center* of \mathfrak{g} and its elements are called Casimir functions.

The Casimir invariants of the Poisson manifold \mathcal{V}_N form the center of the Lie algebra $C^\infty(\mathcal{V}_N)$. Hence they are independent of the dynamics and only depend on the Poisson structure of the manifold, in particular its degeneracy. We are interested in Hamiltonian systems characterized by globally conserved quantities, such as energy, angular momentum, vorticity, etc. Hence, we assume that \mathcal{V}_N is a *regular* Poisson manifold, namely $\text{rank}(\mathcal{J}_N(u)) = 2R$, for all $u \in \mathcal{V}_N$, with $R \in \mathbb{N}$, $2R \leq N$.

Reduced basis methods for dynamical systems, designed with the goal of preserving the algebraic and geometric structure of the phase flow, need to rely on time integrators which preserve the Poisson structure of the phase space. While the literature on canonically symplectic temporal integrators is vast, for the case of Poisson systems with non-constant structure, general structure-preserving methods are largely unavailable, cf. e.g. [27] for a comprehensive discussion of the topic. The study of geometric numerical integrators for general Poisson structures is, however, an active area of research. There exist Poisson temporal integrators tailored to specific differential equations: an example is provided by the symplectic Euler method and partitioned Lobatto IIIA-IIIIB method which preserve the Poisson structure of the Volterra lattice equation and the Ablowitz-Ladik discrete formulation of the nonlinear Schrödinger equation. Since the study of geometric numerical integrators is outside of the scope of the present work, we assume henceforth the availability of a Poisson solver for the dynamical system (1.1).

2.2 Canonical Form of Poisson Structures

In the theory of Hamiltonian systems of classical mechanics, canonical forms on cotangent bundles are of great relevance. Resorting to a coordinate system, canonical symplectic structures can be characterized as in the following result.

Proposition 2.7 ([1, Proposition 3.3.21]). *Let $(\mathcal{V}_{2R}, \omega)$ be a symplectic manifold and (U, ψ) a cotangent coordinate chart $\psi(u) = (q^1(u), \dots, q^R(u), p_1(u), \dots, p_R(u))$, for all $u \in U$. Then (U, ψ) is a symplectic canonical chart if and only if $\{q^i, q^j\} = \{p_i, p_j\} = 0$, and $\{q^i, p_j\} = \delta_{i,j}$ on U for all $i, j = 1, \dots, R$, where $\{\cdot, \cdot\}$ is the Poisson bracket on $(\mathcal{V}_{2R}, \omega)$.*

Every finite-dimensional symplectic manifold admits local coordinates in which the local symplectic form is canonical. This result is known as Darboux's theorem [20].

Theorem 2.8. *Let \mathcal{V}_{2R} be a finite $2R$ -dimensional symplectic manifold. For each $u \in \mathcal{V}_{2R}$ there exists a chart (\mathcal{B}_u, Ψ_u) in which a nondegenerate closed 2-form is locally isomorphic to the canonical form. The manifold \mathcal{V}_{2R} can be covered by such charts.*

Note that this result can be extended to the infinite-dimensional case only under special assumptions and in general not if the symplectic structure ω on the manifold is only *weakly* nondegenerate, i.e. the map ω_X^b is injective but not necessarily onto. We refer to [42, 33, 39] for further details on the topic.

To derive the canonical form of Poisson structures one has to first deal with the kernel of the vector bundle map. Every Poisson manifold can be foliated by injectively immersed submanifolds corresponding to the equivalence classes under the following relation: two points on a Poisson manifold belong to the same class if there exists a piecewise smooth curve joining them and comprising segments of integral curves of Hamiltonian vector fields.

Definition 2.9 (Manifold Foliation). Let \mathcal{V}_N be an N -dimensional manifold. A *foliation* F of class C^p and of dimension q on \mathcal{V}_N is a decomposition of \mathcal{V}_N into disjoint connected subsets $F = \{f_\alpha\}_\alpha$, called the *leaves* of the foliation, with the following property: each point of \mathcal{V}_N has a neighborhood \mathcal{B} and a system of C^p coordinates $\mathcal{B} \rightarrow z := (z_s, z_c) \in \mathbb{R}^q \times \mathbb{R}^{N-q}$ such that for each leaf f_α , the components of $\mathcal{B} \cap f_\alpha$ are described by the equations $(z_c)_1 = \text{constant}, \dots, (z_c)_{N-q} = \text{constant}$.

The embedding of each symplectic leaf in a Poisson manifold is an injective Poisson map, and the phase flow of a Hamiltonian vector field preserves the symplectic structures on the leaves.

The combination of Darboux's theorem with the foliation properties of Poisson manifolds (*cf.* also the symplectic stratification theory [4, Chapter 2]) provides a way to bring degenerate Poisson structures into canonical form.

Theorem 2.10 (Lie-Weinstein Splitting Theorem [31, 43]). *Let $(\mathcal{V}_N, \{\cdot, \cdot\}_N)$ be an N -dimensional Poisson manifold. For each $u \in \mathcal{V}_N$ there exists a neighborhood $\mathcal{B}_u \subset \mathcal{V}_N$ of u , in which the rank of \mathcal{V}_N is equal to $2R$, and an isomorphism $\Psi_u : \mathcal{B}_u \rightarrow \mathcal{S} \times \mathcal{N}^1$ where $\mathcal{S} = \Psi_s(\mathcal{B}_u)$ is a symplectic manifold and $\mathcal{N} = \Psi_c(\mathcal{B}_u)$ is a Poisson manifold whose rank vanishes at $\Psi_c(u)$. The factors \mathcal{S} and \mathcal{N} are unique up to local isomorphisms. Moreover, there exist local coordinates $\{q^1, \dots, q^R, p_1, \dots, p_R, c^1, \dots, c^{N-2R}\}$ which are canonical, i.e. $\{q^i, q^j\}_N = \{p_i, p_j\}_N = \{q^i, c^k\}_N = \{p_i, c^k\}_N = 0$, and $\{q^i, p_j\}_N = \delta_{i,j}$ for all $i, j = 1, \dots, R$ and $k = 1, \dots, N - 2R$.*

On the neighborhood \mathcal{B}_u , the coordinates $\{c^k\}_{k=1}^{N-2R}$ correspond to the Casimir invariants, whereas $\{(q^i, p_j)\}_{i,j=1}^R$ are the symplectic canonical coordinates, sometimes referred to as Clebsch variables [16]. In the canonical coordinates, the vector bundle map (2.1) takes the form

$$\mathcal{J}_N^c := \begin{pmatrix} & \text{Id} \\ -\text{Id} & \\ & \\ & 0 \end{pmatrix} : T^*\mathcal{V}_R \times T^*\mathcal{V}_R \times T^*\mathcal{V}_{N-2R} \longrightarrow T\mathcal{V}_N, \quad (2.4)$$

where Id and 0 denote the identity and zero map, respectively.

There are many advantages for using canonical coordinates, see e.g. [39]. Most prominently, the possibility of bringing the Poisson tensor into constant-valued form and isolate its kernel. The design of the structure-preserving reduced basis methods for (1.1), proposed in this work, hinges upon canonical forms obtained via exact or approximate Darboux maps, *cf.* Sections 3.1 and 4.1.

2.3 Construction of Global Darboux's Map

On finite-dimensional Poisson manifolds \mathcal{V}_N , endowed with a *constant-valued* Poisson structure \mathcal{J}_N , the Darboux map from Theorem 2.8 is global. An analytic expression for the Darboux map can be derived by reverting to well-known results on matrix decompositions.

¹The Cartesian product of two Poisson manifolds is endowed with a Poisson structure given by the Poisson map property of the projection on each factor, and by requiring that the pullbacks of the Poisson algebras on each factor form commuting subalgebras of the Poisson algebra of the Cartesian product.

Proposition 2.11. *Every skew-symmetric matrix $M \in \mathbb{R}^{N,N}$ with $\text{rank}(M) = 2R < N$ admits a decomposition of the form*

$$M = U \mathcal{J}_N^c U^\top, \quad (2.5)$$

where $U \in \mathbb{R}^{N,N}$ is invertible (but not orthogonal in general), and $\mathcal{J}_N^c \in \mathbb{R}^{N,N}$ is the matrix representation of the Poisson tensor in canonical form, namely

$$\mathcal{J}_N^c := \begin{pmatrix} \mathcal{J}_{2R}^c & 0_{2R,q} \\ 0_{q,2R} & 0_q \end{pmatrix}, \quad \mathcal{J}_{2R}^c := \begin{pmatrix} 0_R & I_R \\ -I_R & 0_R \end{pmatrix},$$

where $q := N - 2R$ is the dimension of the null space of M , $0_R \in \mathbb{R}^{R,R}$ and $I_R \in \mathbb{R}^{R,R}$ denote the zero and the identity matrix, respectively.

The factorization (2.5) is unique up to transformations in the symplectic group $\text{Sp}(2R, \mathbb{R})$.

Proof. We propose a constructive proof in three steps: The implementation on the numerical experiments of Section 5 will mimic the arguments.

Step 1. Every skew-symmetric square matrix can be brought into canonical form by a unitary congruence transformation, i.e. there exists $Q \in \mathbb{R}^{N,N}$ orthogonal such that $M = QSQ^\top$. The so-called Youla form S [46] is formed by blocks along the main diagonal, each 2×2 block formed by the complex part of a conjugate pair of complex eigenvalues of M , $\{\pm i\delta_j\}_{j=1}^R$, $\delta_j > 0$, and zeros for $j > R$. The proof of this result can be found in [46, Corollary 2] or [23, Theorem 2].

The Youla decomposition is not unique: the factor S can be fixed by computing a decomposition for a given ordering of the eigenvalues of M , see e.g. [10]. However, the orthogonal matrix Q is not unique.

Step 2. The block diagonal matrix $S \in \mathbb{R}^{N,N}$ can be further decomposed as $S = \hat{D}\hat{S}\hat{D}$ where the matrix \hat{D} is diagonal with diagonal equal to $(\sqrt{\delta_1}, \sqrt{\delta_1}, \dots, \sqrt{\delta_R}, \sqrt{\delta_R}, 0, \dots, 0)$, while each element of $\hat{S} \in \mathbb{R}^{N,N}$ is the sign of the corresponding element of S , i.e. the upper left block $\hat{S}_{2R} \in \mathbb{R}^{2R,2R}$ of S is formed by R blocks along the main diagonal, each 2×2 block containing ± 1 as off-diagonal elements. Combining the first two steps, one has $M = Q\hat{D}\hat{S}\hat{D}Q^\top$.

Step 3. As a last step, we construct a permutation matrix such that \hat{S}_{2R} is similar to \mathcal{J}_{2R}^c . Let $\hat{P}_{2R} \in \mathbb{R}^{2R,2R}$ be the perfect shuffle permutation matrix in \mathbb{R}^{2R} , i.e.

$$\hat{P}_{2R} := [e_1 | e_3 | \dots | e_{2R-1} | e_2 | e_4 | \dots | e_{2R}],$$

where e_j is the j -th canonical column vector in \mathbb{R}^{2R} . Then $\hat{S}_{2R} = \hat{P}_{2R}\mathcal{J}_{2R}^c\hat{P}_{2R}^\top$, and we have that $M = Q\hat{D}\hat{P}\mathcal{J}_N^c\hat{P}^\top\hat{D}Q^\top$, where $\hat{P} \in \mathbb{R}^{N,N}$ is the zero extension of \hat{P}_{2R} .

Since we seek a transformation that brings M into canonical form and is invertible, we introduce the modified matrices

$$D := \begin{pmatrix} \hat{D}_{2R} & 0_{2R,q} \\ 0_{q,2R} & I_q \end{pmatrix}, \quad P := \begin{pmatrix} \hat{P}_{2R} & 0_{2R,q} \\ 0_{q,2R} & I_q \end{pmatrix}. \quad (2.6)$$

The matrices D and P are invertible, and the extension of \hat{P}_{2R} by the identity I_q makes P into an orthogonal matrix. With the modified matrices P and D , the decomposition still holds, namely $M = QDP\mathcal{J}_N^cP^\top DQ^\top$. The conclusion (2.5) follows by setting $U = QDP$.

It can be easily verified that the factorization is not unique: if $Y \in \mathbb{R}^{N,N}$ satisfies $Y\mathcal{J}_N^cY^\top = \mathcal{J}_N^c$ and it is nonsingular, then (2.5) holds with UY in lieu of U . \square

3 Constant-Valued Degenerate Poisson Structures

Although the major challenge in developing reduced basis methods for general Hamiltonian systems manifests itself in the presence of non-constant Poisson tensors, tackling the degeneracy of the structure first, paves the way to the general case. Therefore, in this Section we develop reduced basis methods for parametric Hamiltonian systems on Poisson manifolds with a constant-valued Poisson structure. In the general non-constant case, treated in Section 4, the approach developed and studied here becomes important locally.

To fix the notation, \mathcal{V}_N is assumed to be an N -dimensional Poisson manifold with bracket $\{\cdot, \cdot\}_N$ and constant-valued tensor \mathcal{J}_N with $\text{rank}(\mathcal{J}_N) = 2R$. Moreover, \mathcal{V}_N is regarded as a submanifold of \mathbb{R}^N equipped with the standard Euclidean metric whose induced norm is denoted henceforth by $\|\cdot\|$.

3.1 Splitting of Poisson Dynamics

We recast the dynamical system (1.1) using a suitable coordinate system on \mathcal{V}_N as follows. Let $\mathcal{T} := (t_0, T]$ be a temporal interval and let \mathcal{V}_N be an N -dimensional Poisson manifold with Poisson tensor $\mathcal{J}_N(u)$. For each parameter η in the compact set $\Lambda \subset \mathbb{R}^d$, we consider the initial value problem: For $u_0(\eta) \in \mathcal{V}_N$, find $u(\cdot, \eta) \in C^1(\mathcal{T}, \mathcal{V}_N)$ such that

$$\begin{cases} \partial_t u(t, \eta) = \mathcal{J}_N \nabla \mathcal{H}_N(u(t, \eta); \eta), & \text{for } t \in \mathcal{T}, \\ u(t_0, \eta) = u_0(\eta). \end{cases} \quad (3.1)$$

To ensure well-posedness of (3.1), we assume that, for any $\eta \in \Lambda$, $\nabla \mathcal{H}_N$ is Lipschitz continuous in u in the $\|\cdot\|$ -norm, uniformly in $t \in \mathcal{T}$.

As a first step towards the development of reduced basis methods for (3.1), we perform a *global* splitting of the Poisson manifold $(\mathcal{V}_N, \mathcal{J}_N)$, following Section 2.2, as

$$\Psi : \mathcal{V}_N \longrightarrow \mathcal{V}_{2R} \times \mathcal{N},$$

where $\mathcal{V}_{2R} = \Psi_s(\mathcal{V}_N)$ is a symplectic manifold of dimension $2R$ and $\mathcal{N} = \Psi_c(\mathcal{V}_N)$ is a submanifold whose dimension equals q , the number of independent Casimir invariants of $\{\cdot, \cdot\}_N$. The map Ψ exists, is linear and bijective in view of Proposition 2.11, and satisfies $\Psi \mathcal{J}_N \Psi^\top = \mathcal{J}_{\mathcal{N}}^c$. The splitting preserves the Poisson structure of \mathcal{V}_N .

Proposition 3.1. *Let $\{\cdot, \cdot\}_{cN} : C^\infty(\mathcal{V}_N) \times C^\infty(\mathcal{V}_N) \rightarrow C^\infty(\mathcal{V}_N)$ be the bracket defined by $\{\mathcal{F}, \mathcal{G}\}_{cN}(u) := \nabla \mathcal{F}(u)^\top \mathcal{J}_{\mathcal{N}}^c \nabla \mathcal{G}(u)$, for all $\mathcal{F}, \mathcal{G} \in C^\infty(\mathcal{V}_N)$ and $u \in \mathcal{V}_N$. The manifold $(\mathcal{V}_N, \{\cdot, \cdot\}_{cN})$ is Poisson. Moreover, the map $\Psi : (\mathcal{V}_N, \{\cdot, \cdot\}_N) \rightarrow (\mathcal{V}_N, \{\cdot, \cdot\}_{cN})$ and its inverse are Poisson.*

Proof. It can be easily verified that the operator $\mathcal{J}_{\mathcal{N}}^c$ satisfies the assumptions of Lemma 2.2 and therefore it is a Poisson structure.

To prove that the map $\Psi : (\mathcal{V}_N, \{\cdot, \cdot\}_N) \rightarrow (\mathcal{V}_N, \{\cdot, \cdot\}_{cN})$ is Poisson we need to show that $(\Psi^* \{\mathcal{F}, \mathcal{G}\}_{cN})(u) = \{\Psi^* \mathcal{F}, \Psi^* \mathcal{G}\}_N(u)$, for all $u \in \mathcal{V}_N$ and $\mathcal{F}, \mathcal{G} \in C^\infty(\mathcal{V}_N)$; thereby,

$$\begin{aligned} \{\Psi^* \mathcal{F}, \Psi^* \mathcal{G}\}_N(u) &= \nabla(\Psi^* \mathcal{F})(u)^\top \mathcal{J}_N \nabla(\Psi^* \mathcal{G})(u) = (\Psi^* \nabla \mathcal{F})(u)^\top \mathcal{J}_N (\Psi^* \nabla \mathcal{G})(u) \\ &= (\nabla \mathcal{F})(\Psi u)^\top \Psi \mathcal{J}_N \Psi^\top (\nabla \mathcal{G})(\Psi u) = (\nabla \mathcal{F})(\Psi u)^\top \mathcal{J}_{\mathcal{N}}^c (\nabla \mathcal{G})(\Psi u) \\ &= \{\mathcal{F}, \mathcal{G}\}_{cN}(\Psi u). \end{aligned}$$

An analogous reasoning shows that $((\Psi^{-1})^* \{\mathcal{F}, \mathcal{G}\}_N)(u) = \{(\Psi^{-1})^* \mathcal{F}, (\Psi^{-1})^* \mathcal{G}\}_{cN}(u)$ for all $u \in \mathcal{V}_N$ and $\mathcal{F}, \mathcal{G} \in C^\infty(\mathcal{V}_N)$. \square

The dynamics $\Phi_{X_{\mathcal{H}_N}}^t$ can then be decoupled into the dynamics on the symplectic leaf and the trivial dynamics of the Casimir invariants, i.e. (3.1) can be recast in canonical form as: Find $z(\cdot, \eta) \in C^1(\mathcal{T}, \mathcal{V}_N)$ such that

$$\begin{cases} \partial_t z(t, \eta) = \mathcal{J}_{\mathcal{N}}^c \nabla \mathcal{H}_{\mathcal{N}}^c(z(t, \eta); \eta), & \text{for } t \in \mathcal{T}, \\ z(t_0, \eta) = \Psi u_0(\eta), \end{cases} \quad (3.2)$$

where $\mathcal{H}_{\mathcal{N}}^c := (\Psi^{-1})^* \mathcal{H}_N$ for every $\eta \in \Lambda$ and the canonical Poisson tensor $\mathcal{J}_{\mathcal{N}}^c$ (2.4).

Since Ψ is linear and bijective, Proposition 3.1 implies that Ψ is a Poisson isomorphism: for any $t \in \mathcal{T}$ and any fixed parameter $\eta \in \Lambda$, $z(t, \eta)$ is a solution to (3.2) if and only if $z(t, \eta) = \Psi u(t, \eta)$, where $u(t, \eta)$ is a solution of (3.1).

Moreover, since Poisson maps preserve the Poisson bracket, the invariants of $\Phi_{X_{\mathcal{H}_N}}^t$ are in one-to-one correspondence with the invariants of $\Phi_{X_{\mathcal{H}_{\mathcal{N}}^c}}^t$.

Corollary 3.2. *For any fixed parameter $\eta \in \Lambda$, let $\Phi_{X_{\mathcal{H}_N}}^t$ and $\Phi_{X_{\mathcal{H}_N^c}}^t$ be the flow maps associated with (3.1) and (3.2), respectively. The function $\mathcal{I} \in C^\infty(\mathcal{V}_N)$ is an invariant of motion of $\Phi_{X_{\mathcal{H}_N}}^t$ if and only if $(\Psi^{-1})^*\mathcal{I} \in C^\infty(\mathcal{V}_N)$ is an invariant of $\Phi_{X_{\mathcal{H}_N^c}}^t$. Conversely, $\mathcal{I} \in C^\infty(\mathcal{V}_N)$ is an invariant of motion of $\Phi_{X_{\mathcal{H}_N^c}}^t$ if and only if $\Psi^*\mathcal{I} \in C^\infty(\mathcal{V}_N)$ is an invariant of $\Phi_{X_{\mathcal{H}_N}}^t$.*

Note that all *independent* Casimir invariants of a constant-valued degenerate Poisson tensor are linear. Indeed the Casimir invariants of $\{\cdot, \cdot\}_{cN}$ are the functions $\{\mathcal{I}_m : z \in \mathcal{V}_N \mapsto z_m := (\Psi_c u)_m\}_{m=1}^q$. In view of Proposition 3.1 and Corollary 3.2, the functions $\{\Psi^*\mathcal{I}_m\}_m$ are Casimir invariants of $\{\cdot, \cdot\}_N$ and since Ψ is linear, they are linear in u .

3.2 Reduced Basis Methods Preserving Poisson Structures

By exploiting the splitting of the dynamics, introduced in Section 3.1, we seek a structure-preserving symplectic model order reduction on the symplectic manifold \mathcal{V}_{2R} , while leaving unchanged the submanifold \mathcal{N} associated with the center of the Lie algebra $C^\infty(\mathcal{V}_N)$.

The reduced basis solution is the linear combination of a suitably chosen finite collection of solution trajectories, computed from the high-fidelity model in canonical form, to provide an optimal decomposition in the sense of representing the dominant components of the dynamics. This is done via a weak greedy strategy, discussed in Section 3.2.2. The reduced basis functions are constructed to span an n -dimensional vector space \mathcal{V}_n , for $n \ll N$, with the following properties:

- \mathcal{V}_n is a manifold endowed with the canonical Poisson structure $\{\cdot, \cdot\}_{cn}$.
- The rank of the canonical Poisson tensor \mathcal{J}_n^c on \mathcal{V}_n , $\text{rank}(\mathcal{J}_n^c) = 2r$, satisfies $n - 2r = q$, namely the dimension of the center of the Lie algebras $C^\infty(\mathcal{V}_N)$ and $C^\infty(\mathcal{V}_n)$ coincides.

To compute the evolution of the coefficients of the expansion in the reduced basis we rely on a Galerkin projection of the original dynamical system (3.1). This ensures that the expansion coefficients are uniquely determined by the basis. To preserve the Poisson structure, the projection is constructed to be symplectic on the symplectic leaf of \mathcal{V}_N and to preserve the kernel of the Poisson tensor \mathcal{J}_N .

Let $\pi_+ : \mathcal{V}_N \rightarrow \mathcal{V}_n$ be a *surjective* map which is assumed to be *linear*. Since π_+ is surjective there exists a linear map $\pi : \mathcal{V}_n \rightarrow \mathcal{V}_N$ such that $\pi_+ \circ \pi : \mathcal{V}_n \rightarrow \text{Im}(\pi) \subset \mathcal{V}_N \rightarrow \mathcal{V}_n$ is the identity on \mathcal{V}_n .

Lemma 3.3. *The map $\pi_+ : (\mathcal{V}_N, \{\cdot, \cdot\}_{cN}) \rightarrow (\mathcal{V}_n, \{\cdot, \cdot\}_{cn})$ is Poisson if and only if*

$$\pi_+ \mathcal{J}_N^c \pi_+^\top = \mathcal{J}_n^c.$$

Proof. We need to show that the pullback of π_+ preserves the Poisson bracket, namely that $(\pi_+^* \{\mathcal{F}, \mathcal{G}\}_{cn})(u) = \{\pi_+^* \mathcal{F}, \pi_+^* \mathcal{G}\}_{cN}(u)$, for all $u \in \mathcal{V}_N$ and $\mathcal{F}, \mathcal{G} \in C^\infty(\mathcal{V}_n)$. Let $y := \pi_+ u$. Rewriting the bracket using the canonical vector bundle map \mathcal{J}_N^c , results in

$$\begin{aligned} \{\pi_+^* \mathcal{F}, \pi_+^* \mathcal{G}\}_{cN}(u) &= \nabla(\pi_+^* \mathcal{F})(u)^\top \mathcal{J}_N^c \nabla(\pi_+^* \mathcal{G})(u) = (\pi_+^* \nabla \mathcal{F})(u)^\top \mathcal{J}_N^c (\pi_+^* \nabla \mathcal{G})(u) \\ &= (\nabla \mathcal{F})(\pi_+ u)^\top \pi_+ \mathcal{J}_N^c \pi_+^\top (\nabla \mathcal{G})(\pi_+ u) = \{\mathcal{F}, \mathcal{G}\}_{cn}(\pi_+ u), \end{aligned}$$

where the last equality holds if and only if $\pi_+ \mathcal{J}_N^c \pi_+^\top = \mathcal{J}_n^c$. □

Following the splitting approach, described in Section 3.1, the map π_+ can be constructed as

$$\pi_+ : \mathcal{V}_{2R} \times \mathcal{N} \longrightarrow \mathcal{V}_{2r} \times \mathcal{N}, \quad \pi_+ = \pi_+^s \times \text{Id},$$

where π_+^s is taken to be a surjective ℓ^2 -orthogonal symplectic map, i.e. $\pi_+^s \mathcal{J}_{2R}^c (\pi_+^s)^\top = \mathcal{J}_{2r}^c$.

Remark 3.4. The map π cannot be a Poisson map between the regular Poisson manifolds $(\mathcal{V}_n, \{\cdot, \cdot\}_{cn})$ and $(\mathcal{V}_N, \{\cdot, \cdot\}_{cN})$. Indeed, if that was the case, by a simple counting argument $\text{rank}(\mathcal{J}_N^c) \leq \min\{\text{rank}(\mathcal{J}_n^c), \text{rank}(\pi)\}$, which cannot hold under the assumption $r \ll R$.

Definition 3.5. The *Poisson projection* onto $\text{Im}(\pi^s) \times \mathcal{N} \subset \mathcal{V}_N$ is defined as the map $\mathcal{P} = \mathcal{P}_s \times \text{Id} : \mathcal{V}_{2R} \times \mathcal{N} \rightarrow \text{Im}(\pi) \times \mathcal{N}$ such that, for any $z_s \in (\mathcal{V}_{2R}, \mathcal{J}_{2R}^c)$,

$$\omega(\mathcal{P}_s z_s - z_s, \xi) = 0, \quad \forall \xi \in \text{Im}(\pi^s),$$

where ω is the canonical symplectic 2-form on the symplectic vector space $(\mathcal{V}_{2R}, \mathcal{J}_{2R}^c)$.

Note that, if the Poisson tensor is not constant, i.e. $\mathcal{J}_N = \mathcal{J}_N(u)$, then $\pi_+ \mathcal{J}_N(u) \pi_+^\top$ is still skew-symmetric for every $u \in \mathcal{V}_N$, but it may not satisfy the Jacobi identity (2.3), in which case π_+ fails to provide a reduced Poisson structure.

The reduced problem is derived via the Poisson projection $\mathcal{P} := \pi \circ \pi_+$ onto $\text{Im}(\pi) \subset \mathcal{V}_N$ of the canonical Poisson dynamical system (3.2), namely for $t \in \mathcal{T}$ and $\eta \in \Lambda$, the approximation $z_{\text{rb}}(t, \eta) \approx z(t, \eta)$ satisfies

$$\partial_t z_{\text{rb}}(t, \eta) = \mathcal{P}(\mathcal{J}_N^c \nabla_z \mathcal{H}_N(\Psi^{-1} z_{\text{rb}}(t, \eta); \eta)), \quad z_{\text{rb}}(t_0, \eta) = z^0(\eta).$$

For $z_{\text{rb}}(t, \eta) = \pi y(t, \eta)$, the function y satisfies

$$\begin{cases} \partial_t y(t, \eta) = \mathcal{J}_n^c \nabla \mathcal{H}_n(y(t, \eta); \eta), & \text{for } t \in \mathcal{T}, \\ y(t_0, \eta) = \pi_+ \Psi u_0(\eta), \end{cases} \quad (3.3)$$

on the n -dimensional Poisson manifold \mathcal{V}_n , where $\mathcal{H}_n := \pi^* \mathcal{H}_N^c$. Problem (3.3) is a dynamical system in canonical Poisson form on the manifold $(\mathcal{V}_n, \mathcal{J}_n^c)$. The assumption on the Lipschitz continuity of $\nabla \mathcal{H}_N$ ensures that $\nabla \mathcal{H}_n$ is also Lipschitz continuous with constant $\|\Psi^{-1}\|^2 L_{\delta \mathcal{H}}^\eta$, where $L_{\delta \mathcal{H}}^\eta$ is the Lipschitz constant of $\nabla \mathcal{H}_N$ for parameter $\eta \in \Lambda$. This guarantees the well-posedness of the reduced problem (3.3).

3.2.1 Stability and Conservation Properties of the Reduced Problem

By construction, the Hamiltonian $\mathcal{H}_n \in C^\infty(\mathcal{V}_n)$ of the reduced systems is obtained by pullback from the Hamiltonian $\mathcal{H}_N^c \in C^\infty(\mathcal{V}_N)$, namely $\mathcal{H}_n = \pi^* \mathcal{H}_N^c$, for all $\eta \in \Lambda$. This has the important consequence that, for any fixed $\eta \in \Lambda$, whenever \mathcal{H}_N is a Lyapunov function with equilibria $\{u_e\}_e$ [1, Chapter 3 p. 207], then \mathcal{H}_N^c is a Lyapunov function with equilibria $\{\Psi u_e\}_e$, and the reduced dynamics preserve the Lyapunov stable equilibria $\{\Psi u_e\}_e$ contained in $\text{Im}(\pi)$. Indeed it can be shown that \mathcal{H}_n is a Lyapunov function with equilibria given by the image of the equilibria of the canonical Poisson system under π_+ .

Concerning the preservation of the invariants of motion of $\Phi_{X_{\mathcal{H}_N^c}}^t$ after the reduction, we introduce the following concepts.

Definition 3.6. The model order reduction described by $\mathcal{P} = \pi \circ \pi_+$ is said to be *invariant-preserving* if the Hamiltonian of the high-fidelity canonical problem (3.2) satisfies $\mathcal{H}_N^c \in \text{Im}(\pi_+^*)$, for all $\eta \in \Lambda$.

A weaker condition is that the error in the Hamiltonian vanishes only along solution trajectories: the model order reduction is said to be *Hamiltonian-preserving* if

$$\Delta \mathcal{H}_N^c(\mathcal{P}, \eta) := |\mathcal{H}_N^c(z(t, \eta); \eta) - \mathcal{H}_N^c(\pi y(t, \eta); \eta)| = 0, \quad \forall t \in \mathcal{T}, \eta \in \Lambda,$$

with z solution of (3.2) and y solution of the reduced problem (3.3).

If the model order reduction is invariant-preserving then $\mathcal{H}_N^c = \pi_+^* \mathcal{H}_n$, since π_+^* is injective.

Note that since the map π_+^* acts as the identity on the center of the Lie algebra $C^\infty(\mathcal{V}_N)$, which is therefore not affected by the reduction, the Casimir invariants of the bracket $\{\cdot, \cdot\}_N$ are exactly conserved in the reduced problem. Moreover, the Poisson map π_+ provides a Hamiltonian-preserving model reduction.

Proposition 3.7. For any $\eta \in \Lambda$ fixed, let $z \in C^1(\mathcal{T}, (\mathcal{V}_N, \mathcal{J}_N^c))$ be a solution of the high-fidelity model (3.2) and $y \in C^1(\mathcal{T}, (\mathcal{V}_n, \mathcal{J}_n^c))$ be a solution of the reduced model (3.3). Then the reduced basis method given by $\mathcal{P} = \pi \circ \pi_+$ is *Hamiltonian-preserving* in the sense of Definition 3.6.

Proof. Since the Hamiltonian is an invariant of motion, it holds

$$\begin{aligned}\Delta \mathcal{H}_N^c(\mathcal{P}, \eta) &= |\mathcal{H}_N^c(z(t, \eta); \eta) - \mathcal{H}_n(y(t, \eta); \eta)| = |\mathcal{H}_N^c(z_0(\eta); \eta) - \mathcal{H}_n(y_0(\eta); \eta)| \\ &= |\mathcal{H}_N^c(z_0(\eta); \eta) - (\pi_+^* \mathcal{H}_n)(z_0(\eta); \eta)|,\end{aligned}$$

for z and y being solutions of (3.2) and (3.3), respectively, with $z_0(\eta) := \Psi u_0(\eta)$. This implies that the reduced model is Hamiltonian-preserving if $z_0(\eta) \in \text{Im}(\pi)$ for all $\eta \in \Lambda$.

Let $\eta \in \Lambda$ be fixed. Introducing the shifted variable $z^p(t; \eta) := z(t; \eta) - z_0(\eta) \in \mathcal{V}_N$ for all $t \in \mathcal{T}$, the high-fidelity canonical problem (3.2) can be cast as

$$\begin{cases} \partial_t z^p(t, \eta) = \mathcal{J}_N^c \nabla \mathcal{H}_N^{c,p}(z^p(t, \eta); \eta), & \text{for } t \in \mathcal{T}, \\ z^p(t_0; \eta) = 0, \end{cases} \quad (3.4)$$

where $\mathcal{H}_N^{c,p}(z^p(t; \eta); \eta) := \mathcal{H}_N^c(z^p(t; \eta) + z_0(\eta); \eta)$ for all $t \in \mathcal{T}$. Let us apply the splitting of the dynamics and the \mathcal{J}_N^c -Poisson reduced basis method, described in the previous Sections, to (3.4): The resulting reduced basis method is Hamiltonian-preserving for every parameter, i.e., $\Delta \mathcal{H}_N^{c,p}(\mathcal{P}, \eta) = 0$ for all $\eta \in \Lambda$. This follows from the fact that the initial condition $z^p(t_0; \eta) = 0 \in \text{Im}(\pi)$ for all $\eta \in \Lambda$ since the map π is linear. Note that the invariants of motion $\{\mathcal{I}_m^p\}_m$, associated with the Hamiltonian vector field of $\mathcal{H}_N^{c,p}$, are in one-to-one correspondence with the invariants $\{\mathcal{I}_m\}_m$ of \mathcal{H}_N^c via $\mathcal{I}_m^p(z) = \mathcal{I}_m(z - z_0)$ for all $z \in \mathcal{V}_N$. \square

With the exception of the Hamiltonian, even if $\mathcal{I} \in C^\infty(\mathcal{V}_N)$ is an invariant of motion of the canonical Poisson system (3.2), $\pi^* \mathcal{I} \in C^\infty(\mathcal{V}_n)$ is not necessarily an invariant of the system (3.3) in $(\mathcal{V}_n, \{\cdot, \cdot\}_{cn})$, since π is not a Poisson map. However, if the reduced model is invariant-preserving, it is possible to characterize the invariants of motion of the high-fidelity model belonging to $\text{Im}(\pi_+^*)$ in terms of the invariants of the reduced dynamical system.

Lemma 3.8. *Let $\eta \in \Lambda$ be fixed. Assume that the model order reduction is invariant-preserving, i.e. $\mathcal{H}_N^c(\cdot, \eta) \in \text{Im}(\pi_+^*)$. Then, $\mathcal{I} \in C^\infty(\mathcal{V}_n)$ is an invariant of $\Phi_{X_{\mathcal{H}_n}}^t$ if and only if $\pi_+^* \mathcal{I} \in C^\infty(\mathcal{V}_N)$ is an invariant of $\Phi_{X_{\mathcal{H}_n^c}}^t$ in $\text{Im}(\pi_+^*) \subset C^\infty(\mathcal{V}_N)$.*

Proof. Let $\widehat{\mathcal{I}} \in C^\infty(\mathcal{V}_N) \cap \text{Im}(\pi_+^*)$ be an invariant of (3.2), and $\widehat{\mathcal{I}} = \pi_+^* \mathcal{I}$. Since π_+^* is injective $\mathcal{I} \in C^\infty(\mathcal{V}_n)$ is unique. We seek to show that the function \mathcal{I} is an invariant of (3.3), i.e., $\{\mathcal{I}, \mathcal{H}_n\}_{cn}(y) = 0$ for all $y \in \mathcal{V}_n$. By the surjectivity of π_+ , there exists at least one $z \in \mathcal{V}_N$ such that $y = \pi_+ z$. Since π_+ is a Poisson map, it holds

$$\{\mathcal{I}, \mathcal{H}_n\}_{cn}(y) = \{\mathcal{I}, \mathcal{H}_n\}_{cn}(\pi_+ z) = (\pi_+^* \{\mathcal{I}, \mathcal{H}_n\}_{cn})(z) = \{\pi_+^* \mathcal{I}, \pi_+^* \mathcal{H}_n\}_N(z) = \{\widehat{\mathcal{I}}, \pi_+^* \mathcal{H}_n\}_N(z).$$

The result follows from the fact that $\mathcal{H}_N^c = \pi_+^* \mathcal{H}_n$ by assumption.

For the reverse implication, assume that $\mathcal{I} \in C^\infty(\mathcal{V}_n)$ is such that $\{\mathcal{I}, \mathcal{H}_n\}_{cn}(y) = 0$ for all $y \in \mathcal{V}_n$. Let $\mathcal{D}(\pi_+)$ be the preimage of π_+ in \mathcal{V}_N . An analogous reasoning yields,

$$0 = \{\mathcal{I}, \mathcal{H}_n\}_{cn}(\pi_+ z) = (\pi_+^* \{\mathcal{I}, \mathcal{H}_n\}_{cn})(z) = \{\pi_+^* \mathcal{I}, \pi_+^* \mathcal{H}_n\}_N(z), \quad \forall z \in \mathcal{D}(\pi_+).$$

Hence, $\pi_+^* \mathcal{I}$ is an invariant of (3.1) in $\text{Im}(\pi_+^*) \subset C^\infty(\mathcal{V}_N)$. \square

3.2.2 Reduced Basis Generation via Symplectic Greedy Algorithm

Following a standard reduced basis approach, we build a set of reduced basis functions from a set of high-fidelity solutions, called *snapshots*. Here, however, we need to explore the symplectic part of the solution manifold in the split form. We define the set of solutions of the dynamical system (3.1) as $\mathcal{U} := \{u(t, \eta) = \Phi_{X_{\mathcal{H}_N^c(\cdot, \eta)}}^t(u_0(\eta)) \in (\mathcal{V}_N, \mathcal{J}_N) : t \in \mathcal{T}, \eta \in \Lambda\}$.

Let us consider a time discretization $\Phi_{h, \eta}^t$ of (3.1) on the uniform partition of \mathcal{T} into $M \in \mathbb{N}$ elements, given by $\mathcal{T}_h := \bigcup_{j \in \Upsilon_h} \mathcal{T}_j$, with $\mathcal{T}_j := (t^j, t^{j+1}]$ and $\Upsilon_h := [0, M) \cap \mathbb{N}$. Let Λ_h be a finite subset of the

parameter set Λ and let $\bar{\Upsilon}_h := [0, M] \cap \mathbb{N}$. Now, consider the following sets of solution trajectories, obtained at sample time instants and parameters:

$$\begin{aligned} \mathcal{U}_N &:= \{u^j(\eta) := \Phi_{h,\eta}^{t^j}(u_0(\eta)), j \in \bar{\Upsilon}_h, \eta \in \Lambda_h\}, & \text{sampled solution set of (3.1);} \\ \mathcal{Z}_N &:= \Psi(\mathcal{U}_N) = \{z^j(\eta) := \Psi u^j(\eta), j \in \bar{\Upsilon}_h, \eta \in \Lambda_h\}, & \text{sampled solution set of (3.2);} \\ \mathcal{Z}_N^s &:= \Psi_s(\mathcal{U}_N) = \{\Psi_s u^j(\eta), j \in \bar{\Upsilon}_h, \eta \in \Lambda_h\}, & \text{symplectic component of } \mathcal{Z}_N. \end{aligned} \quad (3.5)$$

As explained previously, the model order reduction is applied only to the canonical symplectic leaf $(\mathcal{V}_{2R}, \mathcal{J}_{2R}^c)$ of \mathcal{V}_N . Hence, the reduced basis functions are generated from the snapshots in \mathcal{Z}_N^s to form an ℓ^2 -orthogonal and canonically \mathcal{J}_{2R}^c -symplectic set.

Definition 3.9 (Orthosymplectic Basis). Let $(\mathcal{V}_{2R}, \omega)$ be a $2R$ -dimensional symplectic vector space and let ω be the canonical symplectic form. Then the set of vectors $\{e_i\}_{i=1}^{2R}$ is said to be *orthosymplectic* in \mathcal{V}_{2R} if

$$\omega(e_i, e_j) = (\mathcal{J}_{2R}^c)_{i,j}, \quad \text{and} \quad (e_i, e_j) = \delta_{i,j}, \quad \forall i, j = 1 \dots, 2R, \quad (3.6)$$

where (\cdot, \cdot) is the Euclidean inner product and \mathcal{J}_{2R}^c is the canonical symplectic tensor on \mathcal{V}_{2R} .

A subspace of a symplectic vector space $(\mathcal{V}_{2R}, \omega)$ is called *Lagrangian* if it coincides with its symplectic complement in \mathcal{V}_{2R} . Since any basis of a Lagrangian subspace of a symplectic vector space $(\mathcal{V}_{2R}, \omega)$ can be extended to a symplectic basis in $(\mathcal{V}_{2R}, \omega)$, every symplectic vector space admits an orthosymplectic basis. Numerical algorithms to build a canonically symplectic reduced basis include the POD-like strategies developed in [40] (cotangent lift, complex SVD, and nonlinear programming) and the symplectic greedy of [2] which couples a weak greedy strategy to select the snapshots to a symplectic Gram–Schmidt [41] procedure to enforce (3.6). Here we opt for a greedy strategy since it gives us larger leeway in the choice of the orthosymplectic reduced basis when compared to a symplectic POD strategy [40].

The greedy approach consists of building a sequence of nested symplectic manifolds $V_{2k} \subset V_{2r}$ and an orthogonal \mathcal{J}_{2k}^c -symplectic basis by minimizing, at each iteration k , the projection error $\|\mathcal{Z}_N^s - \mathcal{P}_{2k} \mathcal{Z}_N^s\|$ and enforcing the constraints $\pi_+^s \mathcal{J}_{2R}^c (\pi_+^s)^\top = \mathcal{J}_{2r}^c$, and $\pi_+^s (\pi_+^s)^\top = \text{Id}$. In this way the reduced space provides a good approximation of the sampled solution manifold \mathcal{Z}_N^s , whereas the constraints ensure that the dynamics in the lower dimensional space has the canonical orthosymplectic Hamiltonian structure (3.3). For the sake of completeness we report in Algorithm 1 the pseudoalgorithm for the weak greedy approach, adapted from [2, Algorithm 2].

Algorithm 1 Symplectic Greedy. Input: $\{\mathcal{Z}_N^s, z_0, \eta_1, \text{tol}_\gamma, \text{tol}_\delta\}$. Output: π^{2j} .

- 1: Set $j = 1$.
 - 2: Given the initial condition z_0 , and η_1 take $e_1 = z_0(\eta_1) / \|z_0(\eta_1)\|$ and $\pi^{2j} = [e_1, (\mathcal{J}_{2R}^c)^\top e_1]$.
 - 3: Compute the pseudoinverse $\pi_+^{2j} = (\mathcal{J}_{2j}^c)^\top \pi^{2j} \mathcal{J}_{2R}^c$.
 - 4: Compute the error in the symplecticity $\delta_{2j} = \|(\pi^{2j})^\top \mathcal{J}_{2R}^c \pi^{2j} - \mathcal{J}_{2j}^c\|_\infty$.
 - 5: Initialize the maximum projection error $\gamma_{2j}^{\max} = 1$.
 - 6: **while** $j < R$, and $\gamma_{2j}^{\max} > \text{tol}_\gamma$, and $\delta_{2j} < \text{tol}_\delta$ **do**
 - 7: Compute the projection error of all snapshots $\gamma_{2j}(z) = \|z - \pi_+^{2j} \pi^{2j} z\|$, for all $z \in \mathcal{Z}_N^s$.
 - 8: Select the new basis element $z^*(\eta_*) = \text{argmax}_{z \in \mathcal{Z}_N^s} \gamma_{2j}(z)$.
 - 9: Update the maximum projection error $\gamma_{2j}^{\max} = \gamma_{2j}(z^*(\eta_*))$.
 - 10: Apply symplectic Gram–Schmidt to $z^*(\eta_*)$ and normalize $e_{j+1} = z^*(\eta_*) / \|z^*(\eta_*)\|$.
 - 11: $j = j + 1$.
 - 12: Update the matrix $\pi^{2j} = [e_1, \dots, e_j, (\mathcal{J}_{2R}^c)^\top e_1, \dots, (\mathcal{J}_{2R}^c)^\top e_j]$.
 - 13: Compute the pseudoinverse $\pi_+^{2j} = (\mathcal{J}_{2j}^c)^\top \pi^{2j} \mathcal{J}_{2R}^c$.
 - 14: Update the error in the symplecticity $\delta_{2j} = \|(\pi^{2j})^\top \mathcal{J}_{2R}^c \pi^{2j} - \mathcal{J}_{2j}^c\|_\infty$.
 - 15: **end while**
-

Remark 3.10 (A posteriori error estimates). A posteriori error estimates are crucial in reduced basis methods to certify the accuracy of the reduced basis approximation online, and for rigorous and efficient error control in the offline greedy sampling procedure, to allow exploration of much larger subsets of the

parameter domain. In the context of dynamical systems, a posteriori error estimators obtained via adjoint problems or via time integration of residual relations are known to exhibit poor long time behavior, in particular for hyperbolic or singularly perturbed problems [44]. Although we acknowledge the importance of efficient and reliable a posteriori error indicators, especially in a greedy approach, in this work we are mainly concerned with the structure-preserving properties of the reduced basis method.

The approximability properties of the solution sets (3.5) by linear subspaces of lower dimension n can be expressed by the Kolmogorov width [28]. The Kolmogorov n -width of a compact subset \mathcal{U}_N of $(\mathcal{V}_N, \|\cdot\|)$ is defined as

$$d_n(\mathcal{U}_N) := \inf_{\substack{W_n \subset \mathcal{V}_N \\ \dim W_n = n}} \sup_{u \in \mathcal{U}_N} \inf_{w \in W_n} \|u - w\|. \quad (3.7)$$

We can bound the Kolmogorov width of the solution set of the canonical problem (3.2) in terms of the Kolmogorov width of \mathcal{U}_N , independently of the sampling of the temporal and parameter spaces. This is expressed in the following Lemma.

Lemma 3.11. *Let \mathcal{U}_N and \mathcal{Z}_N be the sampled solution sets introduced in (3.5). The Kolmogorov n -width of the solution set \mathcal{Z}_N of the dynamical system (3.2) satisfies*

$$d_n(\mathcal{Z}_N) \leq \frac{1}{\min_{1 \leq j \leq N} \sqrt{|\lambda_j(\mathcal{J}_N)|}} d_n(\mathcal{U}_N),$$

where $\{\lambda_j \in \mathbb{C}\}_{j=1}^N$ are the eigenvalues of the constant-valued Poisson tensor \mathcal{J}_N .

Proof. Let $\Psi : (\mathcal{V}_N, \|\cdot\|, \mathcal{J}_N) \rightarrow (\mathcal{V}_N, \|\cdot\|, \mathcal{J}_N^c)$ be the Darboux map associated with the Poisson tensor \mathcal{J}_N , cf. Proposition 2.11. Since Ψ is a linear bijection between finite-dimensional vector spaces, it is bounded. Therefore the Kolmogorov n -width of $\Psi(\mathcal{U}_N)$ can be bounded as

$$d_n(\Psi(\mathcal{U}_N)) \leq \|\Psi\| d_n(\mathcal{U}_N),$$

where $\|\cdot\|$ denotes the operator 2-norm. Let $U \in \mathbb{R}^{N,N}$ be the matrix representation of the linear map Ψ^{-1} . From Proposition 2.11, Ψ is the composition of linear maps: $U^{-1} = (QDP)^{-1}$ where $Q \in \mathbb{R}^{N,N}$ is orthogonal, $D \in \mathbb{R}^{N,N}$ is diagonal and $P \in \mathbb{R}^{N,N}$ is the extension of a permutation matrix by the identity. Hence, it can be inferred that $\|U^{-1}\| \leq \|D^{-1}\| = \max\{1, \max_{1 \leq j \leq N} 1/\sqrt{|\lambda_j(\mathcal{J}_N)|}\}$, where $\{\lambda_j \in \mathbb{C}\}_{j=1}^N$ are the eigenvalues of the Poisson structure \mathcal{J}_N . Note that each eigenvalue λ_j is of the form $\lambda_j = \pm i\delta_j$ with $\delta_j \geq 0$. Since the modified matrix D in (2.6) is an arbitrary nonsingular extension of the matrix \widehat{D}_{2R} , one could in principle extend \widehat{D}_{2R} by $(\min_j \sqrt{\delta_j}) I_q$. The resulting D is nonsingular and $\|D^{-1}\| = 1/\min_{1 \leq j \leq N} \sqrt{|\lambda_j(\mathcal{J}_N)|}$. \square

Proposition 3.12 (Convergence of the Weak Symplectic Greedy Algorithm). *Let \mathcal{U}_N and \mathcal{Z}_N be the sampled solution sets introduced in (3.5). Assume that \mathcal{U}_N has Kolmogorov n -width $d_n(\mathcal{U}_N)$. Then, the reduced space $\mathcal{V}_n = \mathcal{V}_{2r} \times \mathcal{N}$, with \mathcal{V}_{2r} constructed via Algorithm 1, satisfies*

$$\|z - \mathcal{P}z\| \leq \frac{C 3^{r+1}(r+1)}{\min_{1 \leq j \leq N} \sqrt{|\lambda_j(\mathcal{J}_N)|}} d_n(\mathcal{U}_N), \quad \forall z \in \mathcal{Z}_N,$$

where $C > 0$ is a constant independent of n , r and N .

Proof. The convergence estimates for the weak greedy algorithm, derived in [11] and adapted to the symplectic case in [2, Section 4.1.3], result in

$$\|z_s - \mathcal{P}_s z_s\| \leq C 3^{r+1}(r+1) d_{2r}(\mathcal{Z}_N^s), \quad \forall z_s \in \mathcal{Z}_N^s.$$

Let us define the Kolmogorov n -width of \mathcal{Z}_N , restricted to subspaces of \mathcal{V}_n of the form $\mathcal{V}_{2r} \times \mathcal{N}$, as

$$\widehat{d}_n(\mathcal{Z}_N) := \inf_{\substack{\widehat{W}_n \subset \mathcal{V}_N \\ \dim \widehat{W}_n = n}} \sup_{z \in \mathcal{Z}_N} \inf_{w \in \widehat{W}_n} \|z - w\|,$$

where $\widehat{W}_n := \{w \in \mathcal{V}_n : w = (w_s, \Psi_c u), w_s \in \mathcal{V}_{2r}, u \in \mathcal{V}_N\}$. If $d_{2r}(\mathcal{Z}_N^s)$ denotes the Kolmogorov $2r$ -width (3.7) of the symplectic component of the solution set \mathcal{Z}_N , it holds $d_{2r}(\mathcal{Z}_N^s) = \widehat{d}_n(\mathcal{Z}_N) \leq d_n(\mathcal{Z}_N)$. The definition of the Poisson projection from Definition 3.5 together with Lemma 3.11 yields the conclusion. \square

Note that, depending on the decay of the Kolmogorov width, sharper convergence estimates can be derived [9].

3.3 A Priori Convergence Estimates with DEIM

For projection-based reduced order models, empirical interpolation methods [7] provide well-established techniques to evaluate nonlinear terms at a computational cost proportional to the dimension of the reduced problem.

Consider problem (3.2) in canonical form, for a fixed value of the parameter $\eta \in \Lambda$. Assume that the Hamiltonian vector field $\mathcal{M}_N(z) := \nabla \mathcal{H}_N^c(z; \eta)$ is nonlinear in z . The discrete empirical interpolation method (DEIM) [14] consists in approximating \mathcal{M}_N via its oblique projection onto a low-dimensional space, obtained by sampling \mathcal{M}_N at $m \ll N$ interpolation points, namely

$$\mathcal{M}_N(z) \approx U(P^\top U)^{-1} P^\top \mathcal{M}_N(z), \quad \forall z \in \mathcal{V}_N,$$

where $U \in \mathbb{R}^{N,m}$ is the DEIM basis and $P \in \mathbb{R}^{N,m}$ is the DEIM interpolation points matrix. Coupling a DEIM approximation with the reduced basis scheme of Section 3.2, yields $z(t; \eta) \approx \pi y(t; \eta)$ satisfying

$$\partial_t y(t; \eta) = \mathcal{J}_n^c \pi_+ \mathcal{M}_N(\pi y) \approx \mathcal{J}_n^c \pi_+ U(P^\top U)^{-1} P^\top \mathcal{M}_N(\pi y). \quad (3.8)$$

This evolution problem is Hamiltonian, and hence the reduced method structure-preserving, if and only if the term $\mathcal{M}_n(y) := \pi_+ U(P^\top U)^{-1} P^\top \mathcal{M}_N(\pi y)$ can be written as the gradient of a function on \mathcal{V}_n . In addition, (3.8) corresponds to the reduced Hamiltonian system derived from (3.2) if and only if $\mathcal{M}_n(y) = \nabla \mathcal{H}_n(y; \eta)$. This does not seem easy to achieve, if the DEIM basis U is chosen arbitrarily. In [2, Section 4.2] the authors suggest to take $U^\top = \pi_+$. Unfortunately, even in this case the reduced system is no longer Hamiltonian, unless $\mathcal{M}_N(\pi y; \eta)$ belongs to $\text{Im}(\pi)$ for all $y \in \mathcal{V}_n$. In practice, this implies that by constructing a sufficiently large reduced basis π which also includes snapshots of the nonlinear terms, the reduced dynamics possesses asymptotically (in n) a Hamiltonian structure.

We are not aware of any hyper-reduction method able to *exactly* preserve the Hamiltonian phase space structure during model reduction. Although the efficient treatment of the nonlinear terms is a very important aspect of model order reduction, it seems that the development of structure-preserving hyper-reduction techniques requires a thorough analysis, that is beyond the current work.

In this Section, we perform an a priori convergence analysis of the reduced basis method, developed in Section 3.2, including a DEIM approximation of the nonlinear term with $U^\top = \pi_+$, while being aware of the aforementioned limitation of this choice in terms of Hamiltonian structure preservation.

To this end, we assume that the dynamical system (3.1) can be written as $\nabla \mathcal{H}_N(u; \eta) = \mathcal{L}_N u + \mathcal{M}_N(u)$, where \mathcal{L}_N denotes a linear operator and \mathcal{M}_N a nonlinear operator on \mathcal{V}_N (the dependence of \mathcal{L}_N and \mathcal{M}_N on η is omitted for the sake of readability). Then (3.1) can be recast as

$$\partial_t u(t, \eta) = \mathcal{J}_N \mathcal{L}_N u + \mathcal{J}_N \mathcal{M}_N(u), \quad u(t_0, \eta) = u_0(\eta). \quad (3.9)$$

Analogously, we can rewrite the canonical problem (3.2) as $z(t_0, \eta) = \Psi u_0(\eta)$ and

$$\partial_t z(t, \eta) = \mathcal{J}_N^c \nabla_z \mathcal{H}_N(\Psi^{-1} z(t, \eta); \eta) = \mathcal{J}_N^c \mathcal{L}_N^c z(t, \eta) + \mathcal{J}_N^c \mathcal{M}_N^c(z(t, \eta)),$$

where $\mathcal{L}_N^c := \Psi^{-\top} \mathcal{L}_N \Psi^{-1}$ and $\mathcal{M}_N^c(z) := \Psi^{-\top} \mathcal{M}_N(\Psi^{-1} z)$. The reduced problem (3.3) becomes

$$\begin{aligned} \partial_t y(t, \eta) &= \pi_+ \mathcal{J}_N^c \Psi^{-\top} \mathcal{L}_N \Psi^{-1} \pi y(t, \eta) + \pi_+ \mathcal{J}_N^c \Psi^{-\top} \mathcal{M}_N(\Psi^{-1} \pi y(t, \eta)), \\ &= \mathcal{J}_n^c \mathcal{L}_n y(t, \eta) + \mathcal{J}_n^c \pi^\top \Psi^{-\top} \mathcal{M}_N(\Psi^{-1} \pi y(t, \eta)), \end{aligned}$$

where $\mathcal{L}_n := \pi^\top \Psi^{-\top} \mathcal{L}_N \Psi^{-1} \pi$, and $y(t_0, \eta) = \pi_+ z_0(\eta)$. Adopting a DEIM strategy with $U^\top = \pi_+$ we approximate the nonlinear term as

$$\Psi^{-\top} \mathcal{M}_N(\Psi^{-1} \pi y) \approx \pi_+^\top (P^\top \pi_+^\top)^{-1} P^\top \Psi^{-\top} \mathcal{M}_N(\Psi^{-1} \pi y).$$

The reduced problem thus reads

$$\partial_t y(t, \eta) = \mathcal{J}_n^c \mathcal{L}_n y(t, \eta) + \mathcal{J}_n^c (P^\top \pi_+^\top)^{-1} \mathcal{M}_n(y(t, \eta)), \quad y(t_0, \eta) = \pi_+ z_0(\eta), \quad (3.10)$$

where $\mathcal{M}_n(y) := P^\top \Psi^{-\top} \mathcal{M}_N(\Psi^{-1} \pi y)$.

Taking the cue from the convergence analysis in [15], an a priori error estimate can be derived for the state approximation error between the high-fidelity solution and the reduced solution obtained by applying DEIM to the Poisson systems (3.1) and (3.3), respectively. We derive L^2 -error estimates in both time and parameter space. Note that if no hyper-reduction technique is applied error estimates analogous to the ones in Proposition 3.13 hold with $C_2(T, \alpha(\eta)) \equiv 0$ in (3.11).

Proposition 3.13. *For any given $\eta \in \Lambda$, let $u(\cdot, \eta) \in C^1(\mathcal{T}, (\mathcal{V}_N, \mathcal{J}_N))$ be the solution of (3.9) and let $u_{\text{rb}} := \Psi^{-1} \pi y$ where $y(\cdot, \eta) \in C^1(\mathcal{T}, (\mathcal{V}_n, \mathcal{J}_n^c))$ is the solution of the reduced system (3.10). Assume that for every $\eta \in \Lambda$ the nonlinear operator \mathcal{M}_N is Lipschitz continuous in the norm $\|\cdot\|$ with constant $L_{\mathcal{M}}(\eta)$. Then,*

$$\begin{aligned} \|u - u_{\text{rb}}\|_{L^2(\mathcal{T} \times \Lambda; \mathcal{V}_N)}^2 &\leq \|\Psi^{-1}\| C_1(T, \alpha(\eta)) \|\Psi u - \mathcal{P} \Psi u\|_{L^2(\mathcal{T} \times \Lambda; \mathcal{V}_N)}^2 \\ &\quad + \|\Psi^{-1}\|^2 C_2(T, \alpha(\eta)) \|\mathcal{M}_N(u) - \pi_+^\top \pi_+ \mathcal{M}_N(u)\|_{L^2(\mathcal{T} \times \Lambda; \mathcal{V}_N)}^2, \end{aligned} \quad (3.11)$$

where $\alpha(\eta) := \|\Psi^{-\top} \mathcal{L}_N(\eta) \Psi^{-1}\| + \beta \|\Psi^{-1}\|^2 L_{\mathcal{M}}(\eta)$, and $\beta := \|(P^\top \pi_+^\top)^{-1}\|$, $\Delta \mathcal{T} := |T - t_0|$ and

$$C_1(T, \alpha(\eta)) := 2\Delta \mathcal{T} \max_{\eta \in \Lambda} (\alpha(\eta) (e^{2\alpha(\eta)\Delta \mathcal{T}} - 1) + 1), \quad C_2(T, \alpha(\eta)) := 2\Delta \mathcal{T} \beta^2 \max_{\eta \in \Lambda} (\alpha(\eta)^{-1} (e^{2\alpha(\eta)\Delta \mathcal{T}} - 1)).$$

Proof. The error between the high-fidelity and the reduced solution can be bounded by the reduction error associated with the dynamical system in canonical form. Indeed,

$$\|u - u_{\text{rb}}\|_{L^2(\mathcal{T} \times \Lambda; \mathcal{V}_N)}^2 = \int_{\Lambda} \int_{\mathcal{T}} \|\Psi^{-1}(\Psi u(t, \eta) - \pi y(t, \eta))\| dt d\eta \leq \|\Psi^{-1}\| \|z - \pi y\|_{L^2(\mathcal{T} \times \Lambda; \mathcal{V}_N)}^2, \quad (3.12)$$

where z is the solution of the high-fidelity model in canonical form (3.2) and y is the solution of the reduced problem (3.3).

At each time t and $\eta \in \Lambda$, let $z - \pi y = (z - \mathcal{P}z) + (\mathcal{P}z - \pi y) =: e_p + e_h$. If $W := \pi_+^\top (P^\top \pi_+^\top)^{-1} P^\top$, then

$$\begin{aligned} \partial_t e_h(t, \eta) &= \mathcal{P} \partial_t z(t, \eta) - \pi \partial_t y(t, \eta) = \mathcal{P} \mathcal{J}_N^c(\mathcal{L}_N^c z + \mathcal{M}_N^c(z) - \mathcal{L}_N^c \pi y - W \mathcal{M}_N^c(\pi y)) \\ &= \mathcal{P} \mathcal{J}_N^c \mathcal{L}_N^c e_h + \mathcal{P} \mathcal{J}_N^c \mathcal{L}_N^c e_p + \mathcal{P} \mathcal{J}_N^c (\mathcal{M}_N^c(z) - W \mathcal{M}_N^c(\pi y)) \\ &=: \mathcal{O}(\eta) e_h + \mathcal{Q}(t, \eta). \end{aligned}$$

Using that $(I - W) \pi_+^\top \pi_+ \mathcal{M}_N^c(z) = 0$, we bound \mathcal{Q} as,

$$\begin{aligned} \|\mathcal{Q}(t, \eta)\| &\leq \|\mathcal{L}_N^c e_p\| + \|(I - W) \mathcal{M}_N^c(z)\| + \|W(\mathcal{M}_N^c(z) - \mathcal{M}_N^c(\pi y))\| \\ &\leq \|\mathcal{L}_N^c\| \|e_p\| + \|(I - W)(\mathcal{M}_N^c(z) - \pi_+^\top \pi_+ \mathcal{M}_N^c(z))\| + \|W(\mathcal{M}_N^c(z) - \mathcal{M}_N^c(\pi y))\| \\ &\leq \|\mathcal{L}_N^c\| \|e_p\| + \|I - W\| \|w\| + \|W\| L_{\mathcal{M}}(\eta) \|\Psi^{-1}\|^2 (\|e_p\| + \|e_h\|), \end{aligned}$$

where $w(t, \eta) := \mathcal{M}_N^c(z(t, \eta)) - \pi_+^\top \pi_+ \mathcal{M}_N^c(z(t, \eta))$. The error satisfies the evolution equation

$$\begin{aligned} \partial_t \|e_h\| &= \frac{1}{\|e_h\|} (\partial_t e_h, e_h)_V = \frac{1}{\|e_h\|} (\mathcal{O}(\eta) e_h, e_h)_V + \frac{1}{\|e_h\|} (\mathcal{Q}(t, \eta), e_h)_V \\ &\leq \|\mathcal{O}(\eta)\| \|e_h\| + \|\mathcal{Q}(t, \eta)\| \leq \alpha(\eta) \|e_h\| + b(t, \eta), \end{aligned} \quad (3.13)$$

where $\alpha(\eta) := \|\mathcal{L}_N^c\| + \|W\| L_{\mathcal{M}}(\eta) \|\Psi^{-1}\|^2$ and $b(t, \eta) := \alpha(\eta) \|e_p(t, \eta)\| + \beta \|w(t, \eta)\|$, $\beta := \|I - W\|$. Since W is a projector $\beta = \|I - W\| = \|W\|$: the norm of W is bounded [14, Lemma 3.2], and depends on the DEIM selection of indices in P [14, Section 3.2]. From (3.13), Gronwall's inequality [26] gives

$$\begin{aligned} \|e_h(t, \eta)\| &\leq \|e_h(t_0, \eta)\| e^{\alpha(\eta)t} + \int_{t_0}^t e^{\alpha(\eta)(t-s)} b(s, \eta) ds \\ &\leq \left(\int_{t_0}^t e^{2\alpha(\eta)(t-s)} ds \right)^{1/2} \left(2 \int_{t_0}^t \alpha(\eta)^2 \|e_p(s, \eta)\|^2 + \beta^2 \|w(s, \eta)\|^2 ds \right)^{1/2}. \end{aligned}$$

Hence, for all $t \in \mathcal{T}$,

$$\|e_h(t, \eta)\|^2 \leq c(t, \alpha(\eta)) \int_{t_0}^t (\alpha(\eta))^2 \|e_p(s, \eta)\|^2 + \beta^2 \|w(s, \eta)\|^2 ds,$$

where $c(t, \alpha(\eta)) := 2\alpha(\eta)^{-1}(e^{2\alpha(\eta)(t-t_0)} - 1)$ assuming $\alpha(\eta) \neq 0$, for all $\eta \in \Lambda$. This implies that,

$$\begin{aligned} \|z - \pi y\|_{L^2(\mathcal{T} \times \Lambda; \mathcal{V}_N)}^2 &\leq \int_{\Lambda} \int_{t_0}^T \|e_p(t, \eta)\|^2 dt d\eta \\ &\quad + \Delta\mathcal{T} \int_{\Lambda} c(T, \alpha(\eta)) \int_{t_0}^T (\alpha^2(\eta) \|e_p(t, \eta)\|^2 + \beta^2 \|w(t, \eta)\|^2) dt d\eta \\ &\leq 2\Delta\mathcal{T}\beta^2 \int_{\Lambda} \alpha(\eta)^{-1} (e^{2\alpha(\eta)\Delta\mathcal{T}} - 1) \|\mathcal{M}_N^c(z(\cdot, \eta)) - \pi_+^\top \pi_+ \mathcal{M}_N^c(z(\cdot, \eta))\|_{L^2(\mathcal{T}; \mathcal{V}_N)}^2 d\eta \\ &\quad + \int_{\Lambda} (\Delta\mathcal{T}\alpha(\eta)(e^{2\alpha(\eta)\Delta\mathcal{T}} - 1) + 1) \|z(\cdot, \eta) - \mathcal{P}z(\cdot, \eta)\|_{L^2(\mathcal{T}; \mathcal{V}_N)}^2 d\eta \\ &\leq C_1(T, \alpha(\eta)) \|z - \mathcal{P}z\|_{L^2(\mathcal{T} \times \Lambda; \mathcal{V}_N)}^2 \\ &\quad + \|\Psi^{-1}\| C_2(T, \alpha(\eta)) \|\mathcal{M}_N(\Psi^{-1}z) - \pi_+^\top \pi_+ \mathcal{M}_N(\Psi^{-1}z)\|_{L^2(\mathcal{T} \times \Lambda; \mathcal{V}_N)}^2. \end{aligned}$$

The conclusion follows by combining this with (3.12). \square

A few observations are in order. The projection error appearing in the estimate of Proposition 3.13 can be written as

$$\begin{aligned} \|z - \mathcal{P}z\|_{L^2(\mathcal{T} \times \Lambda; \mathcal{V}_N)}^2 &\leq \left| \|z - \mathcal{P}z\|_{L^2(\mathcal{T} \times \Lambda; \mathcal{V}_N)}^2 - \sum_{j \in \overline{\mathcal{T}}_h, i \leq \#\Lambda} w_{j,i} \|z(t^j, \eta_i) - \mathcal{P}z(t^j, \eta_i)\|^2 \right| \\ &\quad + \sum_{j \in \overline{\mathcal{T}}_h, i \leq \#\Lambda} w_{j,i} \|z(t^j, \eta_i) - \mathcal{P}z(t^j, \eta_i)\|^2. \end{aligned}$$

The term in absolute value is a quadrature error ($\{w_{j,i}\}_{j \in \overline{\mathcal{T}}_h, i \leq \#\Lambda}$ are quadrature weights), and depends on the number and choice of the snapshots \mathcal{Z}_N , the smoothness of the integrand in the temporal variable and in the parameter, etc. The second term is controlled by the greedy algorithm according to Proposition 3.12.

The term $\|\mathcal{M}_N(u) - \pi_+^\top \pi_+ \mathcal{M}_N(u)\|_{L^2(\mathcal{T} \times \Lambda; \mathcal{V}_N)}^2$ in (3.11) can be controlled during the assembling of the reduced basis from the nonlinear snapshots $\{\mathcal{M}_N(u^j(\eta))\}_{j \in \overline{\mathcal{T}}_h, i \leq \#\Lambda}$, see [14, 15, Section 2.1] and [2, Section 4.2].

Finally, observe that the bound in (3.11) depends exponentially on the final time T . A linear dependence on T can be obtained in special cases, e.g. when $\nabla \mathcal{H}_N$ is uniformly negative monotone or when the linear part of (3.9) has a logarithmic norm $\eta(\mathcal{L}_N) := \lim_{h \searrow 0} (\|\text{Id} + h\mathcal{L}_N\| - 1)/h$ [19] bounded by $\|(P^\top \pi_+^\top)^{-1}\|_{L_{\mathcal{M}}}$, as in [15, Sections 3 and 4].

4 State-Dependent Poisson Structures

The Hamiltonian formulation of many nondissipative problems possesses a Poisson structure which is not only degenerate but also depends on the state variable. The most common non-constant Poisson structures are linear on the dual of finite-dimensional Lie algebras, known as the Lie–Poisson structures. The difficulty in dealing with such problems stems from the time dependence and nonlinearity intrinsic to the manifold structure.

As for the constant-valued case, Darboux’s Theorem 2.8 suggests a change of coordinates to bring the structure into a canonical form that is more amenable to discretization and model order reduction. However, in the state-dependent case, the Darboux charts have a local nature and the corresponding global change of coordinates is nonlinear. Hence, aside from very particular cases [32, 35], it is generally non-trivial to derive such maps. In addition, resorting to approximation techniques requires particular

care. Indeed the use of too crude an approximation of the Poisson tensor, e.g., by expanding the state u in a power series of a small parameter and then truncate the expansion of $\mathcal{J}_N(u)$, destroys the underlying Poisson structure since the Jacobi identity (2.3) generally fails to hold for the approximate tensor. In the context of Hamiltonian perturbation theory, [37] advocates a near identity change of variables in the neighborhood of a stable equilibrium to bring the Poisson tensor in constant form pointwise. This approach is, however, limited to weakly nonlinear Hamiltonian systems which describe the dynamics near equilibria, and introduces a local approximation of the Poisson structure by truncating the expansion of the Poisson tensor.

We propose an entirely different approach that leverages the unavoidable approximation, introduced by the temporal integrator, by performing a local approximation of the Darboux map in each discrete time interval and subsequently derive a reduced basis method for the resulting, locally canonical, structure.

To keep the presentation focused, we next consider dynamical systems which do not depend on a parameter, namely

$$\begin{cases} d_t u(t) = \mathcal{J}_N(u(t)) \nabla \mathcal{H}_N(u(t)), & \text{for } t \in \mathcal{T}, \\ u(t_0) = u_0. \end{cases} \quad (4.1)$$

We comment on the extension of the results in the forthcoming Sections to the parameter-dependent case in Section 4.4.

4.1 Local Approximation of Darboux's Charts

We exploit the linearization, introduced by the timestepping, to derive local approximations of the Darboux map Ψ , and construct a partition of \mathcal{V}_N along the solution trajectory, by using linear approximations of the homomorphisms $\{\Psi_u\}$ from Theorem 2.10, on each temporal interval.

On the temporal mesh $\mathcal{T}_h = \bigcup_{j \in \Upsilon_h} \mathcal{T}_j$ the discretization of (4.1) yields: For $u_0 \in \mathcal{V}_N$, find $\{u^{j+1}\}_{j \in \Upsilon_h} \subset \mathcal{V}_N$ such that

$$\begin{cases} u^{j+1} = u^j + \Delta t \mathcal{J}_N(\hat{u}^j) \nabla \mathcal{H}_N(\hat{u}^j), & \text{for } j \in \Upsilon_h, \\ u^0 = u_0, \end{cases} \quad (4.2)$$

where $\hat{u}^j \in \mathcal{V}_N$ is determined by the temporal discretization, and can be a state or a combination of them. Alternative discretizations of the Poisson tensor and the Hamiltonian can be considered. This choice will affect the convergence estimates and the restriction of the time step in Theorem 4.7, but not the approximation of the Darboux map nor the derivation of the reduced basis method.

For each $j \in \Upsilon_h$, let $\mathcal{V}_{N,j}$ be an open subset of \mathcal{V}_N containing the states u^{j+1} , u^j , and \hat{u}^j associated with the discrete problem (4.2).

Definition 4.1. On each submanifold $\mathcal{V}_{N,j}$, with $j \in \Upsilon_h$, the local approximation of the Darboux map Ψ is defined to be a bijective linear function $\psi_{j+1/2} : \mathcal{V}_{N,j} \rightarrow \mathcal{V}_{N,j}$ that satisfies $\psi_{j+1/2} \mathcal{J}_N(\hat{u}^j) \psi_{j+1/2}^\top = \mathcal{J}_N^c$ at the state(s) $\hat{u}^j \in \mathcal{T}_j$ dictated by the temporal discretization (4.2). Each map $\psi_{j+1/2}$ provides the local splitting $\psi_{j+1/2} : \mathcal{V}_{N,j} \rightarrow \mathcal{V}_{2R} \times \mathcal{N}_j$, where \mathcal{N}_j is the approximation of the subspace associated with the kernel of the Poisson tensor at \hat{u}^j .

We define *transition maps* between neighboring subsets as $T_j : \psi_{j-1/2}(\mathcal{V}_{N,j-1} \cap \mathcal{V}_{N,j}) \rightarrow \psi_{j+1/2}(\mathcal{V}_{N,j-1} \cap \mathcal{V}_{N,j})$, with $T_j := \psi_{j+1/2} \circ \psi_{j-1/2}^{-1}$ for $j \in \Upsilon_h \setminus \{0\}$, and $T_0 := \text{Id}$. A sketch of the approximate Darboux's charts is presented in Figure 1.

For any $j \in \Upsilon_h$ fixed, the map $\psi_{j+1/2}$ is in general *not* Poisson on $\mathcal{V}_{N,j}$. However, provided the time discretization (4.2) preserves the Casimir invariants, the collection of maps $\{\psi_{j+1/2}\}_{j \in \Upsilon_h}$ preserves the rank of the Poisson structure since $\dim \mathcal{N}_j = q$ for all $j \in \Upsilon_h$.

With the local change of coordinates introduced by each $\psi_{j+1/2}$, we define $z^{j+1} \in \mathcal{V}_{2R} \times \mathcal{N}_j$ as $z^{j+1} = \psi_{j+1/2} u^{j+1}$, where $u^{j+1} \in \mathcal{V}_N$ is solution of problem (4.2) in \mathcal{T}_j . Then, it can be easily shown that $\{z^{j+1}\}_{j \in \Upsilon_h}$ satisfy

$$\begin{cases} z^{j+1} = T_j z^j + \Delta t \mathcal{J}_N^c \nabla \mathcal{H}_N^j(\hat{z}^j), & \text{for } j \in \Upsilon_h, \\ z^0 = \psi_{1/2} u_0, \end{cases} \quad (4.3)$$

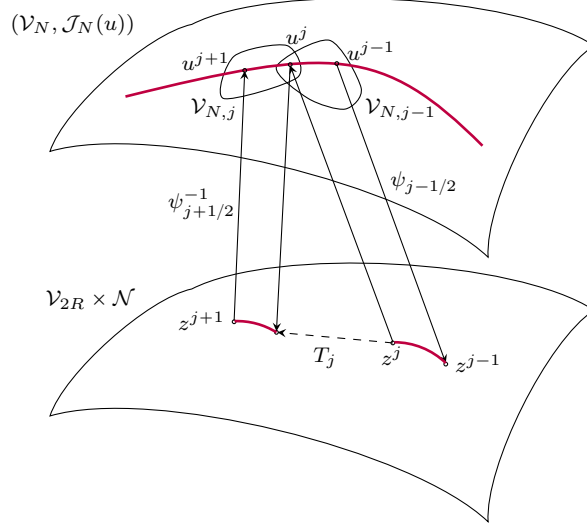


Figure 1: Sketch of Darboux's charts approximation on the Poisson manifold $(\mathcal{V}_N, \mathcal{J}_N(u))$.

where $\widehat{z}^j := \psi_{j+1/2} \widehat{u}^j$ and $\mathcal{H}_N^j(z) := \mathcal{H}_N(\psi_{j+1/2}^{-1} z)$ for all $z \in \mathcal{V}_{N,j}$.

The fact that the approximation of the Darboux map is based on the linearization, introduced by the timestepping, ensures that the Poisson structure is not jeopardized by recasting the discrete problem (4.2) as (4.3). This implies that: $\mathcal{I} \in C^\infty(\mathcal{V}_N)$ is an invariant of the motion of $\Phi_{X_{\mathcal{H}_N}}^t$ if and only if $\mathcal{I}^j := \psi_{j+1/2}^* \mathcal{I} \in C^\infty(\mathcal{V}_N)$ is a (local) invariant of $\Phi_{X_{\mathcal{H}_N^j}}^t$ for all $j \in \Upsilon_h$.

Corollary 4.2. *The Hamiltonian function \mathcal{H}_N of (4.2) is preserved if and only if (4.3) is locally Hamiltonian-preserving i.e. $\mathcal{H}_N^j(z^{j+1}) = \mathcal{H}_N^j(T_j z^j)$ for every $j \in \Upsilon_h$. This holds true for any invariant of motion of $\Phi_{X_{\mathcal{H}_N}}^t$.*

Proof. Let $\{z^j\}_{j \in \Upsilon_h}$ be numerical solutions of (4.3) in each interval \mathcal{T}_j . By construction, it holds that $\mathcal{H}_N^j(z^{j+1}) = \mathcal{H}_N(\psi_{j+1/2}^{-1} z^{j+1}) = \mathcal{H}_N(u^{j+1})$. If (4.3) is locally Hamiltonian-preserving, using the definition of transition maps and the local conservation properties, we recover

$$\begin{aligned} \mathcal{H}_N^j(z^{j+1}) &= \mathcal{H}_N^j(T_j z^j) = \mathcal{H}_N(\psi_{j+1/2}^{-1} T_j z^j) = \mathcal{H}_N(\psi_{j+1/2}^{-1} \psi_{j+1/2} \psi_{j-1/2}^{-1} z^j) = \mathcal{H}_N^{j-1}(z^j) \\ &= \mathcal{H}_N^{j-1}(T_{j-1} z^{j-1}) = \dots = \mathcal{H}_N^0(z^1) = \mathcal{H}_N^0(T_0 z^0) = \mathcal{H}_N(u_0). \end{aligned}$$

Conversely, if (4.2) is (globally) Hamiltonian preserving, then $\mathcal{H}_N(u_0) = \dots = \mathcal{H}_N(u^j) = \mathcal{H}_N(u^{j+1})$ for all $j \in \Upsilon_h$. The conclusion follows from $\mathcal{H}_N(u^j) = \mathcal{H}_N(\psi_{j-1/2}^{-1} z^j) = \mathcal{H}_N(\psi_{j+1/2}^{-1} T_j z^j)$. \square

The global evolution equation for z is not \mathcal{J}_N^c -Poisson, due to the transition between neighboring intervals, notwithstanding that (4.3) is canonically \mathcal{J}_N^c -Poisson on each time interval \mathcal{T}_j . Furthermore, the initial condition $T_j z^j$ on each \mathcal{T}_j does not in general belong to the canonical Poisson manifold $(\mathcal{V}_{N,j}, \mathcal{J}_N^c)$. Likewise the solution z^{j+1} of (4.3) on \mathcal{T}_j in general does not belong to $(\mathcal{V}_{N,j}, \mathcal{J}_N^c)$, i.e., the splitting of the dynamics is clearly not exact. One might consider a ‘‘correction’’ of the initial condition $T_j z^j$ to reduce the distance between $(\mathcal{V}_{N,j}, \mathcal{J}_N^c)$ and the space where the local dynamics is taking place. However, this could introduce an error in the approximation of the solution of the original problem (4.2) and, more importantly, a loss in the preservation of the original Poisson structure $\mathcal{J}_N(u)$, in view of Corollary 4.2. We therefore do not consider this option. This consideration is supported by the observation that the global evolution of z cannot ‘‘drift away’’ from the canonical Poisson manifold $(\mathcal{V}_{N,j}, \mathcal{J}_N^c)$ provided each $\psi_{j+1/2}$ is a sufficiently accurate approximation of the Darboux map Ψ on the whole interval \mathcal{T}_j . Indeed, the distance, measured in the $\|\cdot\|$ -norm, of the solution of (4.3) in \mathcal{T}_j from the canonical Poisson manifold $(\mathcal{V}_N, \mathcal{J}_N^c)$ is bounded by $\|\psi_{j+1/2} u^{j+1} - \Psi(u^{j+1})\|$. This error is local, independent of the dynamics and

of the space-time discretization, and only depends on the approximation properties of each $\psi_{j+1/2}$, which are clearly problem-dependent, but controllable.

4.2 Reduced Basis Methods for State-Dependent Structures

To develop reduced basis methods for the discrete dynamical system (4.2) we can now apply a *local* reduction approach, similar to that in Section 3.2.

As a lower dimensional space we construct an n -dimensional Poisson manifold, $n \ll N$, endowed with the canonical \mathcal{J}_n^c -Poisson bracket such that $n - \text{rank}(\mathcal{J}_n^c) = q$ and the dimension of the null space of $\mathcal{J}_N(u)$ is conserved in the model order reduction. Analogous to the splitting approach in Section 3.1, this is achieved through a *global* linear surjective map π_+ such that, for every $j \in \Upsilon_h$,

$$\pi_+ : \mathcal{V}_{2R} \times \mathcal{N}_j \longrightarrow \mathcal{V}_{2r} \times \mathcal{N}_j, \quad \pi_+ = \pi_+^s \times \text{Id},$$

where π_+^s is taken to be an ℓ^2 -orthogonal symplectic map, i.e., $\pi_+^s \mathcal{J}_{2R}^c (\pi_+^s)^\top = \mathcal{J}_{2r}^c$.

The map $\pi_+ : (\mathcal{V}_N, \{\cdot, \cdot\}_{cN}) \rightarrow (\mathcal{V}_n, \{\cdot, \cdot\}_{cn})$ is Poisson since $\pi_+ \mathcal{J}_N^c \pi_+^\top = \mathcal{J}_n^c$. However, since the set of solution snapshots does not possess a global Poisson structure, the low-dimensional space \mathcal{V}_n is recovered as a linear subspace of \mathcal{V}_N .

Lemma 4.3. *The map $\mathcal{P} = \pi \circ \pi_+ : \mathcal{V}_N \rightarrow \text{Im}(\pi) \subset \mathcal{V}_N$ is ℓ^2 -orthogonal and it is a projection.*

Proof. A straightforward application of the properties of π and of its pseudoinverse π_+ , yields the result. Using $\pi_+ \circ \pi = \text{Id}$ and the surjectivity of π_+ results in $\mathcal{P} \circ \mathcal{P} = \mathcal{P}$.

The ℓ^2 -orthogonality of \mathcal{P} follows from the fact that, by construction, the pseudoinverse π_+^s and the adjoint of π^s coincide. \square

The orthogonality of \mathcal{P} guarantees the inclusion of $\mathcal{V}_n = \text{Im}(\pi)$ in \mathcal{V}_N , and hence the approximation properties of the reduced solution, while the symplecticity of π_+^s ensures that the nontrivial phase flow is a symplectomorphism and that the local kernel $\{\mathcal{N}_j\}_{j \in \Upsilon_h}$ is preserved.

The reduced problem is derived from the canonical Poisson dynamical systems (4.3) by a local Poisson projection onto $\text{Im}(\pi) \cap \mathcal{V}_{N,j} \subset \mathcal{V}_N$. On the n -dimensional Poisson manifold \mathcal{V}_n , the fully discrete problem reads: For $u_0 \in \mathcal{V}_N$, find $\{y^{j+1}\}_{j \in \Upsilon_h} \subset \mathcal{V}_n$ such that

$$\begin{cases} y^{j+1} = \tau_j y^j + \Delta t \mathcal{J}_n^c \nabla \mathcal{H}_n^j(\hat{y}^j), & \text{for } j \in \Upsilon_h, \\ y^0 = \pi_+ \psi_{1/2} u_0, \end{cases} \quad (4.4)$$

where the quantity \hat{y}^j approximates the pseudo-state \hat{z}^j in (4.3) in the sense that $\hat{z}^j \approx \pi \hat{y}^j$, $\mathcal{H}_n^j(y) := \mathcal{H}_N(\psi_{j+1/2}^{-1} \pi y)$ for all $y \in \mathcal{V}_n$, and the reduced transition maps τ_j are defined as $\tau_j := \pi_+ \circ T_j \circ \pi$ for all $j \in \Upsilon_h \setminus \{0\}$, with $\tau_0 := \text{Id}$. A sufficient condition for the well-posedness of (4.4) is that $\nabla \mathcal{H}_N$ is Lipschitz continuous, where \mathcal{H}_N is the Hamiltonian of the high-fidelity problem (4.2).

Problem (4.4) can be seen as the temporal discretization of an evolution equation which is canonically \mathcal{J}_n^c -Poisson on each time interval \mathcal{T}_j . Indeed $y^{j+1} \in \mathcal{V}_n$ is the numerical approximation of the solution of

$$\begin{cases} d_t y = \mathcal{J}_n^c \nabla \mathcal{H}_n^j(y), & \text{for } t \in \mathcal{T}_j, \\ y^0 = \tau_j y^j, \end{cases} \quad (4.5)$$

where $y^j \in \mathcal{V}_n$ is the numerical solution of (4.4) at time t^j . The reduced phase flow is no longer globally Poisson: the Hamiltonian \mathcal{H}_N of the high-fidelity problem (4.1) is conserved up to the approximation error of the local Darboux map.

Proposition 4.4. *Let u_0 be the initial condition of the dynamical system (4.1). For $j \in \Upsilon_h$ fixed, let $u_{\text{rb}}(t^{j+1})$ be the time-continuous solution of the reduced problem given by $u_{\text{rb}}(t^{j+1}) = \psi_{j+1/2}^{-1} \pi y(t^{j+1})$ where $y(t)$ is the solution of (4.5) at time $t \in \mathcal{T}_h$. If the Hamiltonian \mathcal{H}_N of (4.1) is Lipschitz continuous with constant $L_{\mathcal{H}}$ then*

$$|\mathcal{H}_N(u_{\text{rb}}(t^{j+1})) - \mathcal{H}_N(u_0)| \leq L_{\mathcal{H}} \sum_{k=1}^j \|\psi_{k+1/2}^{-1}\| \|\psi_{k-1/2}\| \|T_k - \text{Id}\| \|u_{\text{rb}}(t^k)\|.$$

Proof. Let $y(t^k) \in \mathcal{V}_n$ be the solution of the reduced system (4.5) at time $t^k \in \mathcal{T}_h$. Since the system is locally \mathcal{J}_N^c -Poisson, the Hamiltonian is an invariant of the local motion, namely $\mathcal{H}_n^k(y(t^{k+1})) = \mathcal{H}_N(\psi_{k+1/2}^{-1}\pi y(t^{k+1})) = \mathcal{H}_n^k(\tau_k y(t^k))$. However, the global Hamiltonian \mathcal{H}_N is not preserved at the interface between intervals. Indeed,

$$\begin{aligned} |\mathcal{H}_n^k(\tau_k y(t^k)) - \mathcal{H}_n^{k-1}(y(t^k))| &= \left| \mathcal{H}_N(\psi_{k+1/2}^{-1}\pi\tau_k y(t^k)) - \mathcal{H}_N(\psi_{k-1/2}^{-1}\pi y(t^k)) \right| \\ &= \left| \mathcal{H}_N(\psi_{k+1/2}^{-1}\mathcal{P}T_k\pi y(t^k)) - \mathcal{H}_N(\psi_{k-1/2}^{-1}\pi y(t^k)) \right|. \end{aligned}$$

If $T_k\pi y(t^k) \in \text{Im}(\pi)$ for all $k \in \Upsilon_h$, then $\psi_{k+1/2}^{-1}\mathcal{P}T_k\pi y(t^k) = \psi_{k-1/2}^{-1}T_k^{-1}\mathcal{P}T_k\pi y(t^k) = \psi_{k-1/2}^{-1}\pi y(t^k)$, and, hence, the Hamiltonian would be preserved.

Under the assumption that the Hamiltonian \mathcal{H}_N is Lipschitz continuous with constant $L_{\mathcal{H}}$ it holds,

$$\begin{aligned} |\mathcal{H}_n^k(\tau_k y(t^k)) - \mathcal{H}_n^{k-1}(y(t^k))| &\leq L_{\mathcal{H}} \|\psi_{k+1/2}^{-1}\mathcal{P}T_k\pi y(t^k) - \psi_{k-1/2}^{-1}\pi y(t^k)\| \\ &= L_{\mathcal{H}} \|\psi_{k+1/2}^{-1}\mathcal{P}(T_k - \text{Id})\pi y(t^k) - \psi_{k+1/2}^{-1}(T_k - \text{Id})\mathcal{P}\pi y(t^k)\| \\ &\leq L_{\mathcal{H}} \|\psi_{k+1/2}^{-1}\| \|\psi_{k-1/2}\| \|T_k - \text{Id}\| \|u_{\text{rb}}(t^k)\|. \end{aligned}$$

Hence, the error in the conservation of the Hamiltonian at time t^j can be bounded as

$$\begin{aligned} |\mathcal{H}_N(u_{\text{rb}}(t^j)) - \mathcal{H}_N(u_0)| &= |\mathcal{H}_n^{j-1}(y(t^j)) - \mathcal{H}_N(u_0)| \leq \sum_{k=1}^{j-1} |\mathcal{H}_n^k(y(t^{k+1})) - \mathcal{H}_n^{k-1}(y(t^k))| \\ &\leq \sum_{k=1}^{j-1} |\mathcal{H}_n^k(\tau_k y(t^k)) - \mathcal{H}_n^{k-1}(y(t^k))| \\ &\leq L_{\mathcal{H}} \sum_{k=1}^{j-1} \|\psi_{k+1/2}^{-1}\| \|\psi_{k-1/2}\| \|T_k - \text{Id}\| \|u_{\text{rb}}(t^k)\|. \end{aligned}$$

□

Observe that if the approximate maps $\{\psi_{j+1/2}\}_{j \in \Upsilon_h}$ are constructed to be continuous at the interface between temporal intervals, i.e., such that, for any $j \in \Upsilon_h$, $\psi_{j-1/2}u^j = \psi_{j+1/2}u^j$, where u^j is solution of (4.2), then the evolution problems (4.3) and (4.4) are globally canonically Poisson, $\tau_j y^j = y^j$ in (4.4), and the preservation of the Hamiltonian is exact.

Since, by construction, the map π_+ acts as the identity on \mathcal{N}_j for all $j \in \Upsilon_h$, the approximation of the center of the Lie algebra $C^\infty(\mathcal{V}_N)$ is not affected by the reduction. This means that the error made in the conservation of the Casimir invariants of the bracket $\{\cdot, \cdot\}_N$ is only attributable to the approximation of the Darboux charts.

Concerning the stability properties of the problem, since the Poisson system (4.1) and its canonical form, obtained through Darboux's map, are in one-to-one correspondence, u_e is a Lyapunov stable equilibrium of (4.1) if and only if $\Psi(u_e)$ is a Lyapunov stable equilibrium of the corresponding canonical system. When resorting to the local approximation of Ψ , as introduced in Definition 4.1, Lyapunov stable equilibria are preserved by the discrete problem since, by construction, $\psi_{j-1/2}^{-1}z^j = u^j$ for all $j \in \Upsilon_h$ with u^j as the numerical solution of (4.2) and z^j as the numerical solution of (4.3) in \mathcal{T}_{j-1} . Note that the property of preserving the Lyapunov equilibria at the discrete level depends on the temporal solver, see e.g. [25] and references therein.

Furthermore, if $\Psi^*\mathcal{H}_N$ is a Lyapunov function, a reasoning analogous to the one of Section 3.2.1 allows to show that the global reduced system associated with the exact Darboux map preserves the Lyapunov stable equilibria belonging to $\text{Im}(\pi)$. However, assuming $u_e \in \mathcal{V}_{N,j-1}$, the reduced state $y_e := \pi_+\psi_{j-1/2}u_e \approx \pi_+\Psi(u_e)$ is generally not an equilibrium of (4.4). Ideally one would want to have that $\|\psi_{j-1/2}^{-1}\pi y^j - u_e\|$ is uniformly bounded for all $j \in \Upsilon_h$, where y^j is the numerical solution of (4.4) in \mathcal{T}_{j-1} . It holds

$$\begin{aligned} \|\psi_{j-1/2}^{-1}\pi y^j - u_e\| &= \|\psi_{j-1/2}^{-1}\pi y^j - \Psi^{-1}(\pi y_e)\| \leq \|\psi_{j-1/2}^{-1}(\pi y^j - \pi y_e)\| + \|\psi_{j-1/2}^{-1}\pi y_e - \Psi^{-1}(\pi y_e)\| \\ &\leq \|\psi_{j-1/2}^{-1}\| \|y^j - y_e\| + \|\psi_{j-1/2}^{-1}\pi y_e - \Psi^{-1}(\pi y_e)\|. \end{aligned}$$

The second term is the approximation error of the Darboux map, while the term $\|y^j - y_e\|$ can be bounded by the approximation error associated with solving the reduced problem (4.4) instead of the reduced system obtained from the exact Darboux map Ψ . Although the reduced solution is not guaranteed to belong to an arbitrary small neighborhood of u_e , the term $\|y^j - y_e\|$ does not depend on the reduction but only on the approximation properties of the Darboux map.

4.2.1 Convergence of the Weak Symplectic Greedy Algorithm

For the derivation of the reduced basis, we rely on the weak greedy algorithm, described in Section 3.2.2, with the following modifications. Let $\Phi_{h,N}^t$ be the discrete flow map associated with the temporal discretization of the high-fidelity problem (4.2). A set of snapshots $\mathcal{U}_N = \{u^j = \Phi_{h,N}^{t^j}(u^0), j \in \bar{\Upsilon}_h\}$ is computed together with the linear approximation maps $\{\psi_{j+1/2}\}_{j \in \Upsilon_h}$. The image of each snapshot under the corresponding $\psi_{j+1/2}$ supplies the solution of the local system (4.3) in every time interval. By extracting the symplectic part and excluding the contribution of the Casimir invariants, we define

$$\mathcal{Z}_N^s := \{\psi_{j+1/2}^s u^{j+1}, j \in \Upsilon_h\} \cup \{\psi_{1/2}^s u_0\}, \quad (4.6)$$

where $\psi_{j+1/2}^s(\mathcal{V}_{N,j}) = \mathcal{V}_{2R}$ is a $2R$ -dimensional subspace of \mathcal{V}_N . We finally build an orthogonal \mathcal{J}_{2R}^c -symplectic reduced basis from \mathcal{Z}_N^s via Algorithm 1 and the Poisson projection $\mathcal{P} := \pi \circ \pi_+$ from π^s and π_+ .

Theorem 4.5 (Convergence of the Weak Symplectic Greedy Algorithm). *Let $\Phi_{h,cN}^t$ be the discrete flow map associated with (4.3). Assume that the solution set $\mathcal{Z}_N := \{z^j = \Phi_{h,cN}^{t^j}(z^0), j \in \bar{\Upsilon}_h\}$ has Kolmogorov n -width $d_n(\mathcal{Z}_N)$. Then, the reduced space $\mathcal{V}_n = \mathcal{V}_{2r} \times \mathcal{N}$, with \mathcal{V}_{2r} obtained via the symplectic weak greedy Algorithm 1, satisfies*

$$\|z - \mathcal{P}z\| \leq C3^{r+1}(r+1)d_n(\mathcal{Z}_N), \quad \forall z \in \mathcal{Z}_N,$$

where the finite constant $C > 0$ is independent of n , r and N .

Proof. Let \mathcal{Z}_N^s be the set (4.6) containing the symplectic part of the solution trajectory at time instants $\{t^j\}_{j \in \bar{\Upsilon}_h}$. Algorithm 1 iteratively generates a hierarchy of subspaces of \mathcal{V}_{2R} such that the projection \mathcal{P}_s is ℓ^2 -orthogonal, see Lemma 4.3. In the context of an orthogonal reduced basis generation via a greedy strategy we can revert to the a priori convergence estimates derived in [11] and [9]. The argument proposed here is a straightforward modification of the proof presented in [11, Section 2] by taking into account the form of the orthosymplectic reduced basis (Definition 3.9), and it is therefore relegated to Appendix A. \square

Remark 4.6. We are making the tacit assumption that the Kolmogorov n -width of the solution set \mathcal{Z}_N has a sufficiently fast decay. Unlike the constant case, see Section 3.2.2 and Lemma 3.11, the Kolmogorov width of the solution set \mathcal{Z}_N associated with the system (4.3) *cannot* easily be bounded by the Kolmogorov width of the solution set of the original system (4.2). That would require stronger conditions on the global Darboux map Ψ , see e.g. [17], which are generally not guaranteed by Darboux's Theorem 2.8.

4.3 A Priori Convergence Estimates for the Reduced Solution

For state-dependent Poisson structures we perform model order reduction in a local perspective. We therefore derive a priori estimates for the error between the high-fidelity solution and the reduced solution for the fully discrete system in each temporal interval. The total error at a given time is controlled by the projection error at all the previous time steps.

Note that the error of the reduced solution is computed with respect to the solution of the fully discrete high-fidelity system and not with respect to the exact solution of (4.1). Hence the estimate (4.7) does not include the approximation error ensuing from the temporal discretization.

Theorem 4.7. *Let $j \in \Upsilon_h$ be fixed. Let u^{j+1} be the numerical solution of (4.2) at time t^{j+1} and let u_{rb}^{j+1} be the numerical solution of the reduced problem, obtained as $u_{\text{rb}}^{j+1} = \psi_{j+1/2}^{-1} \pi y^{j+1}$, where y^{j+1} is the solution of (4.4) at time t^{j+1} . Assume that $\nabla \mathcal{H}_N$ is Lipschitz continuous in the $\|\cdot\|$ -norm with constant*

$L_{\delta\mathcal{H}}$. If the numerical discretization of the Hamiltonian in (4.2) is (semi-)implicit, and the time step Δt satisfies

$$\Delta t L_{\delta\mathcal{H}} C_1 \|\psi_{j+1/2}^{-1}\|^2 < 1, \quad \text{for all } j \in \Upsilon_h,$$

where the finite constant $C_1 > 0$ depends only on the discretization of the Hamiltonian, then,

$$\|u^{j+1} - u_{\text{rb}}^{j+1}\| \leq \frac{\|\psi_{j+1/2}^{-1}\|}{1 - \Delta t L_{\delta\mathcal{H}} C_1 \|\psi_{j+1/2}^{-1}\|^2} \left(\|z^{j+1} - \mathcal{P}z^{j+1}\| + \sum_{k=1}^j \gamma_k \beta_k \|z^k - \mathcal{P}z^k\| \right). \quad (4.7)$$

Here $z^k = \psi_{k-1/2} u^k$, $\beta_k := \|T_k - \text{Id}\| + \Delta t L_{\delta\mathcal{H}} C_2 \|\psi_{k+1/2}^{-1}\|^2$, the constant $C_2 > 0$ depends only on the discretization of the Hamiltonian, and

$$\gamma_k := \begin{cases} 1 + \sum_{m=k+1}^j \beta_m, & \text{if } k \leq j-1, \\ 1, & \text{if } k = j. \end{cases}$$

Proof. Let us split the error at time t^j , for $j \in \bar{\Upsilon}_h$, as

$$e^j := z^j - \pi y^j = (z^j - \mathcal{P}z^j) + (\mathcal{P}z^j - \pi y^j) =: e_p^j + e_h^j.$$

Subtracting the reduced problem (4.4) from problem (4.3), the approximation error e_h^{j+1} at time t^{j+1} can be written as,

$$\begin{aligned} e_h^{j+1} &= \mathcal{P}z^{j+1} - \pi y^{j+1} \\ &= e_h^j + \mathcal{P}(T_j - \text{Id})z^j + \pi y^j - \mathcal{P}T_j \pi y^j + \Delta t \mathcal{P} \mathcal{J}_N^c(\nabla \mathcal{H}_N^j(\hat{z}^j) - \nabla \mathcal{H}_N^j(\pi \hat{y}^j)) \\ &= (\text{Id} + \mathcal{P}(T_j - \text{Id}))e_h^j + \mathcal{P}(T_j - \text{Id})e_p^j + \Delta t \mathcal{P} \mathcal{J}_N^c(\nabla \mathcal{H}_N^j(\hat{z}^j) - \nabla \mathcal{H}_N^j(\pi \hat{y}^j)). \end{aligned}$$

The total error at time t^{j+1} is bounded as,

$$\begin{aligned} \|e^{j+1}\| &\leq \|e_p^{j+1}\| + \|e_h^{j+1}\| \\ &\leq \|\text{Id} + \mathcal{P}(T_j - \text{Id})\| \|e_h^j\| + \|\mathcal{P}(T_j - \text{Id})\| \|e_p^j\| + \Delta t \|R_j\| + \|e_p^{j+1}\| \\ &\leq (1 + \|T_j - \text{Id}\|) \|e_h^j\| + \|T_j - \text{Id}\| \|e_p^j\| + \Delta t \|R_j\| + \|e_p^{j+1}\|, \end{aligned} \quad (4.8)$$

where $R_j := \mathcal{P} \mathcal{J}_N^c(\nabla \mathcal{H}_N^j(\hat{z}^j) - \nabla \mathcal{H}_N^j(\pi \hat{y}^j))$. Since $\nabla \mathcal{H}_N$ is Lipschitz continuous by assumption, using the definition of the local Hamiltonian $\mathcal{H}_N^j := (\psi_{j+1/2}^{-1})^* \mathcal{H}_N$, R_j satisfies

$$\begin{aligned} \|R_j\| &\leq \|\nabla \mathcal{H}_N^j(\hat{z}^j) - \nabla \mathcal{H}_N^j(\pi \hat{y}^j)\| \leq L_{\delta\mathcal{H}} \|\psi_{j+1/2}^{-1}\|^2 \|\hat{z}^j - \pi \hat{y}^j\| \\ &\leq L_{\delta\mathcal{H}} C_1 \|\psi_{j+1/2}^{-1}\|^2 \|e^{j+1}\| + L_{\delta\mathcal{H}} C_2 \|\psi_{j+1/2}^{-1}\|^2 \|e^j\|, \end{aligned} \quad (4.9)$$

where the finite non-negative constants C_1 and C_2 depend only on the temporal discretization of (4.2) (e.g. for the implicit Euler scheme $C_1 = 1$ and $C_2 = 0$, for the implicit midpoint rule $C_1 = C_2 = 1/2$, etc.). Hence, the total error at time t^{j+1} satisfies

$$\begin{aligned} \|e^{j+1}\| &\leq \Delta t L_{\delta\mathcal{H}} C_1 \|\psi_{j+1/2}^{-1}\|^2 \|e^{j+1}\| + (1 + \alpha_j + \Delta t L_{\delta\mathcal{H}} C_2 \|\psi_{j+1/2}^{-1}\|^2) \|e_h^j\| \\ &\quad + (\alpha_j + \Delta t L_{\delta\mathcal{H}} C_2 \|\psi_{j+1/2}^{-1}\|^2) \|e_p^j\| + \|e_p^{j+1}\|. \end{aligned}$$

where $\alpha_j := \|T_j - \text{Id}\|$. Under the condition that the time step Δt satisfies $\Delta t L_{\delta\mathcal{H}} C_1 \|\psi_{j+1/2}^{-1}\|^2 < 1$ for all $j \in \Upsilon_h$, the total error at time t^{j+1} is controlled by the projection error e_p^k at all previous time steps $k \leq j+1$; i.e.,

$$\|e^{j+1}\| \leq \frac{1}{1 - \Delta t L_{\delta\mathcal{H}} C_1 \|\psi_{j+1/2}^{-1}\|^2} \left(\sum_{k=1}^j \beta_k \|e_p^k\| + \|e_p^{j+1}\| + \sum_{k=1}^{j-1} \left(\sum_{m=k+1}^j \beta_m \right) \beta_k \|e_p^k\| \right),$$

where $\beta_m := \alpha_m + \Delta t L_{\delta\mathcal{H}} C_2 \|\psi_{m+1/2}^{-1}\|^2$.

The conclusion follows from the fact that $u^j - u_{\text{rb}}^j = \psi_{j-1/2}^{-1} e^j$. \square

Observe that, except for the evaluation of the nonlinear terms, the local reduced basis technique, described in the previous sections, does not incur a computational cost proportional to N during the online phase since the evaluation of the reduced transition maps $\{\tau_j\}_j$ can be performed offline.

4.4 Parametric State-Dependent Poisson Structures

If we consider a parametric dynamical system similar to (3.1) but with state-dependent Poisson structure, we can extend the derivation and analysis of the reduced basis method described in the previous Sections. The main obstacle relates to the fact that the resolution of the dynamical system in the low-dimensional space (4.4) requires the knowledge of the Darboux map approximations $\{\psi_{j+1/2}\}_j$. These will inevitably depend on the parameter where the Poisson tensor is evaluated. Only the linear maps $\{\psi_{j+1/2}(\eta)\}_j$ associated with the parameters $\eta \in \Lambda_h \subset \Lambda$ will be computed in the offline phase. Therefore a way to approximate each $\psi_{j+1/2}$ at any given parameter $\eta \in \Lambda$ is indispensable.

5 Numerical Experiments

To validate the theoretical results of the previous Sections we perform a set of numerical tests. For lack of Poisson integrators for general structures, we consider ad hoc test cases for which such integrators are available. The rationale is that we seek to assess the performances of the structure-preserving reduced basis method in the absence of pollution from the temporal discretization. Moreover, with the aim of assessing the structure-preserving properties of the proposed model order reduction and for want of structure-preserving hyper-reduction techniques, we test the proposed reduced basis method coupled to the DEIM algorithm only in one numerical experiment (Section 5.1.3).

In the forthcoming numerical simulations, if not otherwise specified, we will use a Newton's method as the nonlinear solver for implicit temporal discretizations. We fix the Newton tolerance to 10^{-10} and the maximum number of nonlinear iterations to 50. In the symplectic greedy Algorithm 1, we consider a stabilized version of the symplectic Gram–Schmidt and a symplectic Gram–Schmidt with full reorthogonalization [24] to deal with cases where the snapshots matrix is ill conditioned.

5.1 Numerical Experiments for Constant-Valued Degenerate Structures

As example of constant-valued degenerate Poisson structure we consider the Korteweg–de Vries (KdV) equation. KdV type problems are nonlinear hyperbolic equations which describe the propagation of waves in nonlinear dispersive media. The KdV equation in the one-dimensional spatial domain Ω and time interval \mathcal{T} reads: Find $u(t, x) : \mathcal{T} \times \Omega \rightarrow \mathbb{R}$ such that

$$\partial_t u + \alpha u \partial_x u + \eta \partial_{xxx}^3 u = 0, \quad \alpha, \eta \in \mathbb{R}. \quad (5.1)$$

The dispersive third order term provides a regularization yielding smooth solutions for smooth initial conditions. The numerical treatment of (5.1) for small values of η , the so-called dispersion limit, is particularly challenging, and for $\eta = 0$, Burgers' equation is recovered.

The KdV equation is a completely integrable system, i.e. it has as an infinite set of invariants, and possesses a bi-Hamiltonian structure: The formulation with a degenerate constant-valued Poisson tensor reads

$$\partial_t u = \mathcal{J} \delta \mathcal{H}(u), \quad \text{with} \quad \mathcal{H}(u) = \int_{\Omega} \left(\frac{\alpha}{6} u^3 - \frac{\eta}{2} (\partial_x u)^2 \right) dx, \quad \mathcal{J} = \partial_x,$$

where δ denotes a functional derivative. Let us consider a uniform partition of the interval $\Omega = [a, b]$, $a, b \in \mathbb{R}$ with periodic boundary conditions, into $N-1$ elements, and let $\Delta x = |b-a|/(N-1)$. The Poisson tensor \mathcal{J} is discretized using centered finite differences, whereas the Hamiltonian \mathcal{H} is approximated using the trapezoidal rule and forward finite differences for the first order spatial derivative, as in [5, Eq. (2)]. With a small abuse of notation, u denotes henceforth the semi-discrete solution. If u_k is the nodal value of u at the k -th mesh node, then

$$\mathcal{H}_N(u) = \Delta x \sum_{k=1}^N \left(\frac{\alpha}{6} u_k^3 - \frac{\eta}{2} \left(\frac{u_{k+1} - u_k}{\Delta x} \right)^2 \right), \quad (5.2)$$

and $(\mathcal{J}_N u)_k = u_{k+1} - u_{k-1}$, for $k = 1, \dots, N$ with $u_{N+k} = u_{1+k}$, $u_0 = u_{N-1}$ by periodicity. Observe that the finite-dimensional operator \mathcal{J}_N ensuing from the discretization of $\mathcal{J} = \partial_x$ is Poisson in the sense of Lemma 2.2. Indeed, the skew-symmetry is guaranteed by using a *centered* finite difference approximation, while the Jacobi identity is satisfied by any constant-valued operator. Moreover, the Poisson tensor \mathcal{J}_N has $\text{rank}(\mathcal{J}_N) = 2R$, with $2R = N - 1$ if N odd, $2R = N - 2$ if N even. The corresponding Casimir invariants are

$$\mathcal{C}_1(u) = \sum_{k=1}^N u_k, \quad \mathcal{C}_2(u) = \sum_{k=1}^N (u_{2k} - u_{2k+1}). \quad (5.3)$$

Note that, if N is odd, then $\mathcal{C}_2(u) \equiv 0$ and \mathcal{C}_1 is the only Casimir invariant of the Poisson system.

Time discretization based on the fully implicit midpoint rule on $\mathcal{T}_h = \bigcup_{j \in \Upsilon_h} [t^j, t^{j+1}]$ yields

$$u^{j+1} - u^j = \frac{\Delta t}{2\Delta x} \mathcal{J}_N \nabla \mathcal{H}_N(u^{j+1/2}), \quad u^0 = \Pi_h u_0, \quad j \in \Upsilon_h, \quad (5.4)$$

where $u^{j+1/2} := (u^{j+1} + u^j)/2$ and Π_h is the nodal interpolation. The implicit midpoint rule provides a Poisson integrator for any constant-valued Poisson tensor. However, it does not preserve the discrete Hamiltonian (5.2) exactly.

As an alternative scheme, we consider the Average Vector Field (AVF) integration [36], which is second order accurate, preserves the Hamiltonian exactly [18, Theorem 3.1], but it is not a Poisson integrator [13]. For $j \in \Upsilon_h$, the fully discrete scheme reads

$$u^{j+1} - u^j = \frac{\alpha}{6} \frac{\Delta t}{2\Delta x} \mathcal{J}_N \left((u^j)^2 + u^j u^{j+1} + (u^{j+1})^2 \right) + \frac{\eta}{2\Delta x^3} \mathcal{J}_N \mathcal{F}_h(u^{j+1/2}), \quad (5.5)$$

with $u^0 = \Pi_h u_0$ and where $(\mathcal{F}_h(u))_k := (u_{k+1} - 2u_k + u_{k-1})/2$, for $k = 1, \dots, N$.

5.1.1 KdV: Long Time Stability of Double Soliton Interaction

To assess the stability of the reduced basis algorithm, we run a numerical test simulating solitons interaction over long time. Let us consider the KdV problem (5.1), with fixed parameters $\alpha = 6$ and $\eta = 1$, in the domain $\Omega = [-20, 20]$ and temporal interval $\mathcal{T} = (0, 100]$. Let the initial condition be the periodic function $u_0(x) = 6 \text{sech}^2(x)$, $x \in \Omega$. The spatial discretization of the high-fidelity problem relies on the finite difference scheme (5.2) with $N = 1000$ mesh nodes. We compare the results obtained with the midpoint rule (5.4) as timestepping and the AVF scheme (5.5), both with uniform time step $\Delta t = 10^{-3}$. We select $M_s = 10000$ snapshots from the high-fidelity solution and run the symplectic greedy Algorithm 1 with tolerances $\text{tol}_\sigma = 10^{-5}$ and $\text{tol}_\delta = 10^{-12}$. The algorithm reaches convergence with $2r = 328$ for the AVF timestepping and $2r = 330$ for the midpoint rule. The need of a sufficiently large reduced space is typical of problems exhibiting propagation phenomena and is associated with a slowly decaying Kolmogorov n -width [21].

The high-fidelity solution and the reduced solution at final time are shown in Figure 2 (left), where the subscripts a and m refer to the AVF scheme and midpoint rule, respectively. The reduced solutions do not present spurious oscillations, not even over long time, and exhibit a qualitatively correct behavior in terms of phase and amplitude of the solitons, as it can be checked by comparing with [6, Example 5.2]. The solution obtained with the midpoint rule is slightly shifted with respect to the solution of the AVF scheme. This is a typical effect of numerical dispersion: the shape of the solitons is preserved but the solution is subject to a phase shift so that the solitons are wrongly located.

The error of the reduced numerical solution with respect to the high-fidelity is reported in Figure 2 (right), where both the original problem (3.1) and its canonical formulation (3.2) are considered. Figure 3 reports the error of the Hamiltonian and of the Casimir invariants (5.3) over time. The AVF scheme (left) ensures almost exact preservation of the Hamiltonian and of the Casimir invariants when the canonical system is solved. For the original high-fidelity model, the Hamiltonian is conserved up to the Newton solver tolerance. The midpoint rule (Figure 3 right) preserves the linear Casimir invariants but not the (cubic) Hamiltonian, as expected.

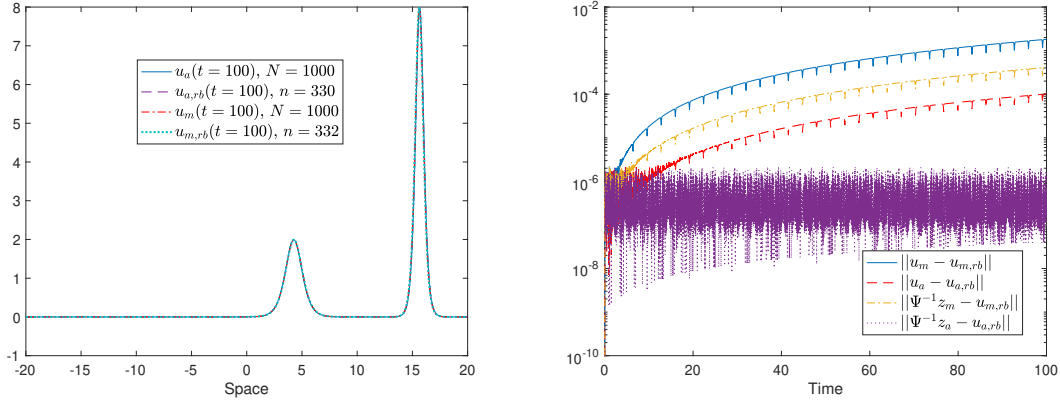


Figure 2: KdV double soliton interaction. Numerical solutions of the high-fidelity and reduced models at final time (left) for AVF timestepping and midpoint rule. Error between the numerical solution of the reduced problem and the high-fidelity solutions of the Poisson system in the original and canonical forms (right).

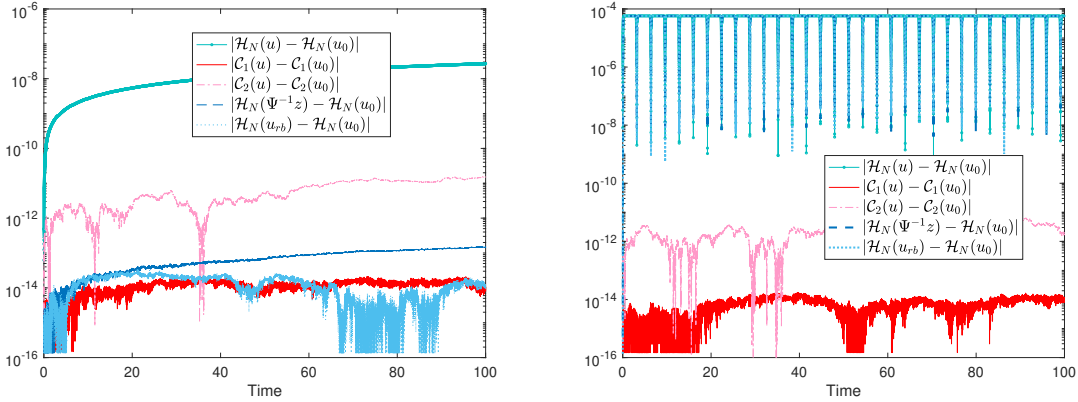


Figure 3: KdV double soliton interaction. Error of the Hamiltonian and Casimir invariants over time. Temporal discretization with AVF scheme (left) and midpoint rule (right).

5.1.2 Parametric KdV: Dispersion Limit

As a second test case, let us consider the KdV equation with varying parameter η and solve the problem in the limit of small dispersion. Specifically, let $\alpha = 1$ and $\eta \in \Lambda := [10^{-6}, 2]$. The problem is set in the domain $\Omega = [0, 1]$ and in the time interval $\mathcal{T} = (0, 1]$ with initial condition $u_0(x) = 2 + 1/2 \sin(2\pi(x - \eta))$, $x \in \Omega$, (a shifted variation of the test in [45, Section 4.6]). The spatial discretization relies on $N = 1600$ mesh nodes, and for the temporal approximation we use the AVF scheme (5.5) with uniform time step $\Delta t = 10^{-3}$. The kernel of the Poisson tensor has dimension $q = 2$. We select $M_s = 500$ snapshots from the high-fidelity model, and Λ_h is obtained by taking 10 equidistant points in Λ . The reduced basis algorithm uses the symplectic greedy Algorithm 1 with tolerances $\text{tol}_\sigma = 10^{-5}$ and $\text{tol}_\delta = 10^{-12}$. Convergence is reached at $2r = 556$.

The reduced solution for $\eta = 10^{-5} \notin \Lambda_h$ captures the train of soliton waves without unphysical oscillations, as shown in Figure 4. The ℓ^2 -error over time of the reduced numerical solution with respect to the high-fidelity solution, obtained from the Poisson system in the non-canonical and canonical forms, is reported in Figure 5 (left). Concerning the invariants of motion, the Hamiltonian of both (4.1) and (3.3) is conserved up to the solver tolerance, Figure 5 (right).

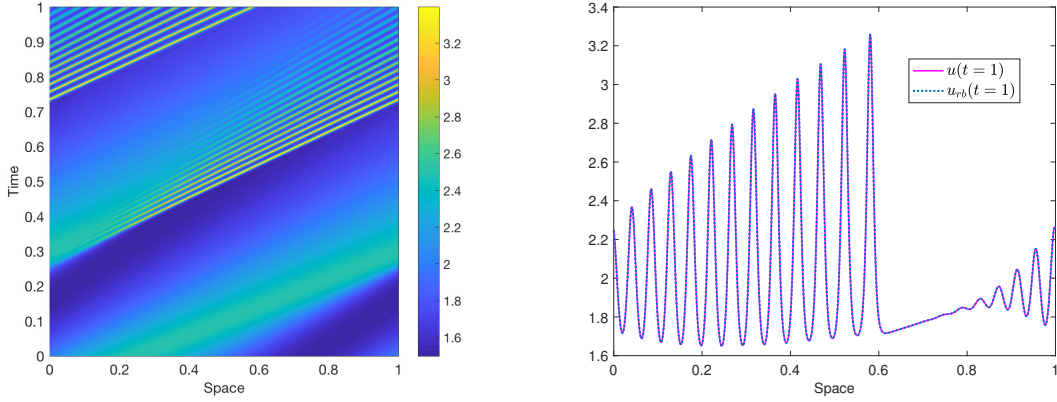


Figure 4: KdV in the dispersion limit, $\eta = 10^{-5}$. Evolution of the solution (left) and solution at final time (right) obtained with the AVF timestepping.

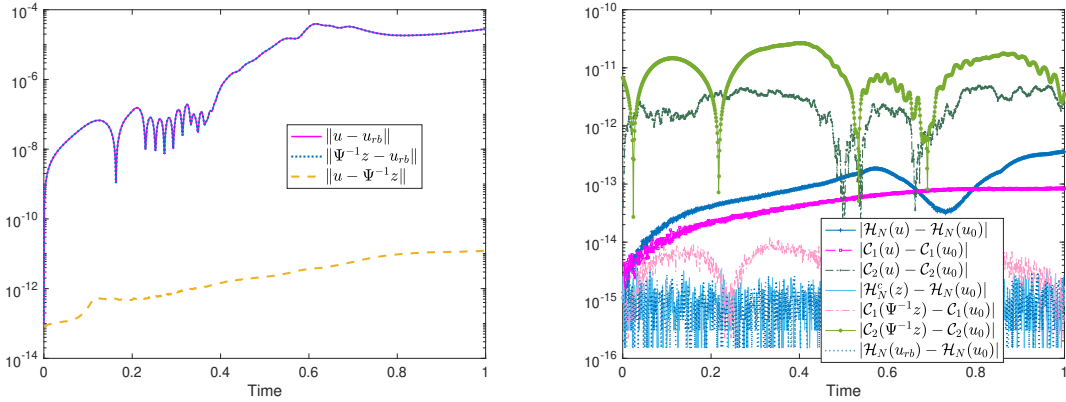


Figure 5: KdV in the dispersion limit, $\eta = 10^{-5}$. Error between the high-fidelity solution and the reduced solution (left). Relative error of the Hamiltonian and the Casimir invariants (right).

As can be observed in the proposed numerical tests, the structure-preserving approach proposed in this work provides robust and efficient reduced methods. However, in order to achieve sufficient accuracy, the reduced models still require relatively large approximation spaces. This is not a limitation of the method but can be ascribed to the *local* low-rank nature of nondissipative phenomena, like advection and wave-type problems, characterized by slowly decaying Kolmogorov n -widths, as shown in [21] for families of 1D transport equations. This behavior can be observed in Figure 6, on the left, where we report the decay of the singular values of the matrix containing the snapshots of the solution of the full model at $M_s = 500$ equispaced temporal instants and for all values of the parameter $\eta \in \Lambda_h$. On the right plot, we report the ℓ^2 -error between the high-fidelity and the reduced solution at final time T versus the runtime required to solve the reduced problem in the online phase at one instance of the parameter η (here $\eta = 10^{-5} \notin \Lambda_h$). The reported runtime does not include the collection of snapshots in the offline phase. The dashed line identifies the runtime of the high-fidelity solver. We can infer that, although a relatively large basis is needed to achieve sufficiently small approximation errors, the reduced model can still be solved at a reduced computational cost as compared to the high-fidelity problem. The observed time saving becomes particularly significant when many-query simulations are considered.

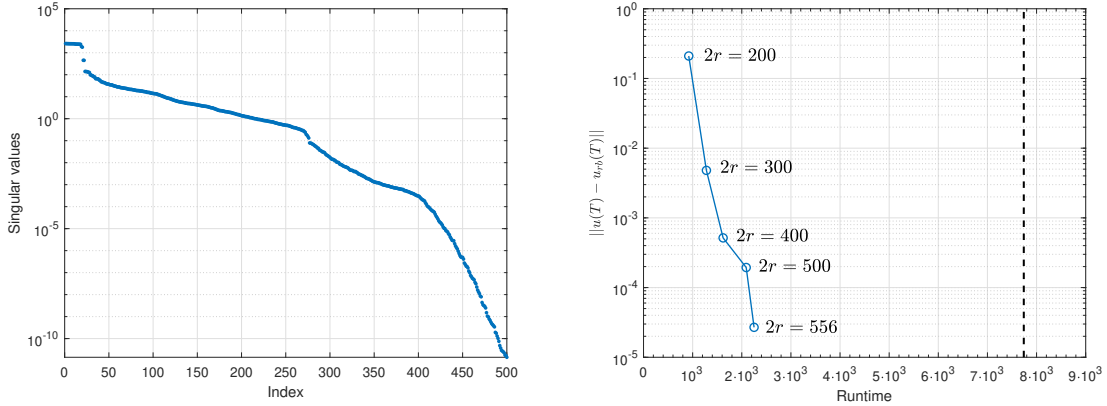


Figure 6: KdV in the dispersion limit. On the left plot, singular values of the snapshot matrix. On the right plot, ℓ^2 -error at final time between the high-fidelity and reduced solution vs. the runtime of the reduced model (online phase) for different values of the reduced basis. The dashed line represents the runtime required by the high-fidelity solver to compute the solution for the parameter $\eta = 10^{-5}$.

5.1.3 KdV in the Dispersion Limit: Reduced Basis Method with DEIM

To achieve computational costs for the solution of the reduced models independent of the dimension of the full model, hyper-reduction techniques are usually employed to approximate nonlinear operators. As discussed in Section 3.3, suitable DEIM strategies have proven to be effective and robust in the model order reduction of Hamiltonian systems, although they are not provably structure-preserving. As a numerical evidence of this fact, we consider the KdV problem (5.1) with fixed dispersion coefficient $\eta = 10^{-5}$. The discretization and model reduction parameters are set as in Section 5.1.2. We denote with u_{DEIM} the reduced solution obtained with our structure-preserving RBM coupled with the DEIM approach of Section 3.3 and with u_{rb} the reduced solution obtained without hyper-reduction.

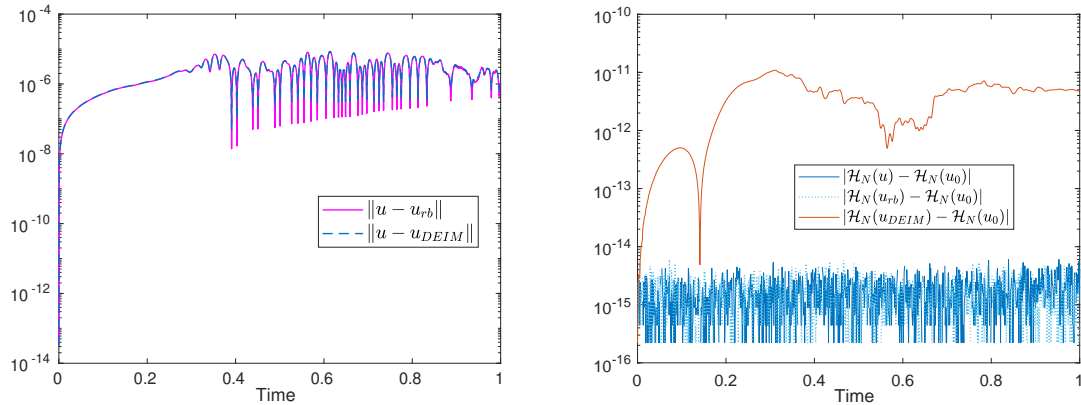


Figure 7: On the left plot, evolution of the ℓ^2 -error between the high-fidelity and the reduced solution with and without DEIM hyper-reduction. On the right plot, evolution of the error in the conservation of the Hamiltonian. Dimension of the reduced space $2n = 558$.

The numerical results obtained when the size of the reduced basis is $2n = 558$ are shown in Figure 7. We can infer that the high-fidelity solution is well-approximated by both reduced models implying that, in this test, the loss of the symplectic structure associated with DEIM does not yield unstable solutions. As it can be observed in Figure 7 on the right, although the Hamiltonian is not exactly preserved by the DEIM approximation, as expected, its error is controlled and does not grow significantly in time. The reason is

that, with a sufficiently large reduced basis, the nonlinear Hamiltonian vector is well-approximated by the DEIM (oblique) projection and the loss of Poisson structure in the reduced phase space is compensated by a highly accurate approximation.

5.2 Numerical Experiments for State-Dependent Structures

The multi-species generalized Lotka–Volterra problem provides an example of a Hamiltonian system with a state-dependent degenerate Poisson structure. The Volterra lattice equation was introduced to describe the interaction and evolution of populations of competing species. Additionally, it provides a discretization of the KdV equation or of the Logistic equation and can be used to model nonlinear control systems, lattice problems, etc. The generalized Lotka–Volterra model for N species reads

$$d_t u_k(t) = u_k(t) \left(b_k + \sum_{\ell=1}^N a_{k,\ell} u_\ell(t) \right), \quad k = 1, \dots, N, \quad b_k, a_{k,\ell} \in \mathbb{R},$$

where $u_{k+N} = u_k$ for all k , for periodic boundary conditions. Here we take the values of $\{b_k\}_k$ and $\{a_{k,\ell}\}_{k,\ell}$ such that

$$d_t u_k = u_k(u_{k+1} - u_{k-1}), \quad k = 1, \dots, N, \quad u_0 = u_N, \quad u_{N+1} = u_1. \quad (5.6)$$

The Lotka–Volterra system (5.6) possesses the invariants

$$\mathcal{I}_q(u) = \sum_{k=1}^N \left(\frac{1}{2} u_k^2 + u_k u_{k+1} \right), \quad \mathcal{I}_c(u) = \sum_{k=1}^N \frac{1}{3} u_k^3 + \sum_{k=1}^N u_k u_{k+1} (u_k + u_{k+1} + u_{k+2}),$$

and the Casimir

$$\mathcal{C}_1(u) = \sum_{k=1}^N \log(u_k).$$

Furthermore, if the number N of species is even, the problem can be recast in a split form as follows. Let $q_k(t) = u_{2k-1}(t)$ and $p_k(t) = u_{2k}(t)$ for $k = 1, \dots, N/2$ and $t \in \mathcal{T}$, then (5.6) is equivalent to

$$\begin{cases} d_t q_k = q_k(p_k - p_{k-1}), \\ d_t p_k = p_k(q_{k+1} - q_k). \end{cases}$$

This is a Poisson system with Hamiltonian $\mathcal{H}_N(q, p) = \sum_{k=1}^{N/2} (q_k + p_k)$, and a quadratic bracket corresponding to the Poisson tensor

$$\mathcal{J}_N(u) := \begin{pmatrix} 0 & q_1 p_1 & & & & & & & -q_1 p_M \\ -q_1 p_1 & 0 & q_2 p_1 & & & & & & \\ & -q_2 p_1 & 0 & q_2 p_2 & & & & & \\ & & -q_2 p_2 & 0 & q_3 p_2 & & & & \\ & & & -q_3 p_2 & 0 & q_3 p_3 & & & \\ & & & & \ddots & \ddots & \ddots & & \\ & & & & & -q_M p_{M-1} & 0 & q_M p_M & \\ q_1 p_M & & & & & & -q_M p_M & 0 & \end{pmatrix},$$

where $M := N/2$. The dimension of the null space is $q = 2$ for all $u \in \mathcal{V}_N$.

Concerning the temporal discretization of the Lotka–Volterra problem in Hamiltonian form, the symplectic Euler method preserves the quadratic Poisson structure [22], and reads, for all $k = 1, \dots, N/2$ and $j \in \Upsilon_h$,

$$\begin{cases} q_k^{j+1} = q_k^j + \Delta t q_k^j (p_k^{j+1} - p_{k-1}^{j+1}), \\ p_k^{j+1} = p_k^j + \Delta t p_k^{j+1} (q_{k+1}^j - q_k^j). \end{cases} \quad (5.7)$$

Let us consider a numerical simulation of problem (5.6) in the temporal interval $\mathcal{T} = (0, 500]$, with initial condition $u_k(t = 0) = 1 + \text{sech}^2(x_k)/(2N^2)$, where $x_k = -1 + 2(k-1)/N$ for $k = 1, \dots, N$. The high-fidelity model is obtained with $N = 1000$ and the symplectic Euler discretization (5.7) with $\Delta t = 10^{-2}$. In the generation of the orthosymplectic reduced basis, the symplectic greedy Algorithm 1 is run with tolerances $\text{tol}_\sigma = 10^{-5}$ and $\text{tol}_\delta = 10^{-12}$. The algorithm reaches convergence with $2r = 210$.

In Figure 8 are reported the ℓ^2 -error of the high-fidelity and reduced basis solutions at every time step (left), and the error of the Hamiltonian, the Casimir \mathcal{C}_1 and the invariants $\mathcal{I}_q, \mathcal{I}_c$ over time (right). It can be observed that the invariants of motion of the high-fidelity problem are preserved with a high accuracy, similarly to [22, Figure 1]. The reduced solution produces larger, though still satisfactory, errors in the conservation of the invariants which however do not grow in time.

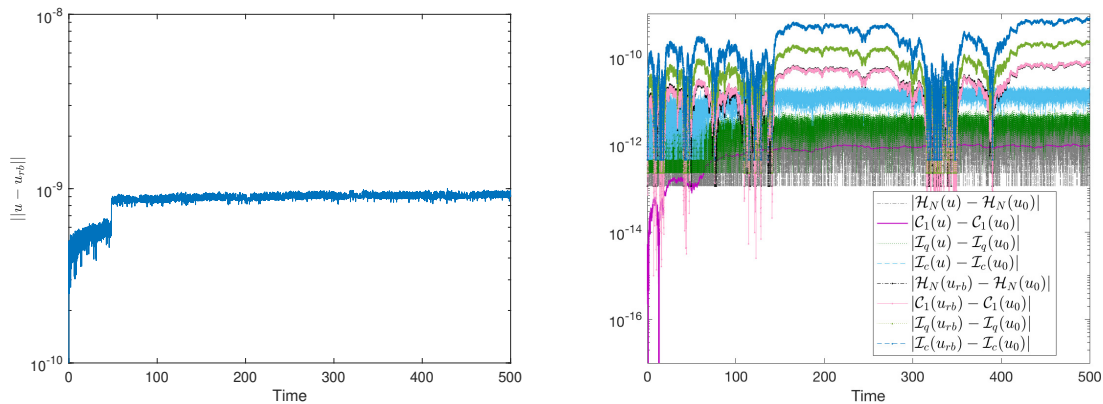


Figure 8: Lotka–Volterra lattice. Evolution of the ℓ^2 -error of the high-fidelity and reduced basis solutions (left). Error in the conservation of the Hamiltonian, the Casimir \mathcal{C}_1 and the invariants $\mathcal{I}_q, \mathcal{I}_c$ over time (right).

6 Concluding Remarks

We have developed and analyzed reduced basis methods for dynamical Hamiltonian systems with a state-dependent and degenerate Poisson structure. The proposed reduced basis techniques are based on “freezing” the Poisson tensor in each temporal interval (or stage) associated with a given temporal discretization, followed by a model order reduction of the symplectic component of the dynamics. We have shown that the resulting reduced model retains the global Poisson structure and the conservation properties of the phase flow up to errors in the approximation of the Darboux map, and enjoys good approximation properties. Further work may target the study of optimal and efficient approximation of the Darboux map, and the corresponding approximation properties in the presence of a set of parameters in addition to time. The development of local-in-time reduced basis methods to more effectively deal with the local low-rank nature of nondissipative phenomena will also be subject of future investigations.

Acknowledgment. This work was partially supported by AFOSR under grant FA9550-17-1-9241.

A Proof of Theorem 4.5

Following Algorithm 1, the reduced basis matrix is initialized as $\pi^2 = [e_1, (\mathcal{J}_{2R}^c)^\top e_1]$ where $e_1 = z_s^0 := \psi_{1/2}^s u_0$. The projection onto $\text{span}\{\pi^2\}$ is defined as $\mathcal{P}_2 = \pi^2 \circ \pi_+^2$ with $\pi_+^2 = (\mathcal{J}_{2,1}^c)^\top \pi^2 \mathcal{J}_{2R}^c$. At the r -th iteration, for $r \geq 1$, the greedy algorithm selects the new basis element e_{r+1} to satisfy

$$e_{r+1} = \operatorname{argmax}_{z \in \mathcal{Z}_N^s} \|z - \mathcal{P}_{2r} z\|,$$

so that $\mathcal{V}_{2(r+1)} = \text{span}\{e_1, \dots, e_{r+1}, (\mathcal{J}_{2R}^c)^\top e_1, \dots, (\mathcal{J}_{2R}^c)^\top e_{r+1}\}$. The basis vectors are orthogonalized with respect to the ℓ^2 -norm as

$$\begin{aligned} \xi_1 &= e_1, \\ \xi_i &= e_i - \mathcal{P}_{2(i-1)} e_i, \quad \xi_{r+i} = (\mathcal{J}_{2R}^c)^\top \xi_i, \quad i = 2, \dots, r+1. \end{aligned}$$

The projection \mathcal{P}_{2r} onto the symplectic manifold \mathcal{V}_{2r} can be written as

$$\mathcal{P}_{2r} z = \sum_{i=1}^r (\alpha_i(z) \xi_i + \beta_i(z) (\mathcal{J}_{2R}^c)^\top \xi_i), \quad \forall z \in \mathcal{Z}_N^s.$$

With \mathcal{Z}_N^s being a subspace of the normed space $(\mathcal{V}_{2R}, \|\cdot\|)$, \mathcal{P}_{2r} is, in view of Lemma 4.3, an orthogonal projection onto \mathcal{V}_{2r} . Hence, for each $z \in \mathcal{Z}_N^s$, $\xi_\ell \in \mathcal{V}_{2r}$ and $\ell \leq r$,

$$\begin{aligned} (\mathcal{P}_{2r} z, \xi_\ell) &= (z, \mathcal{P}_{2r} \xi_\ell) = (z, \xi_\ell) = \alpha_\ell(z) \|\xi_\ell\|^2, \\ (\mathcal{P}_{2r} z, (\mathcal{J}_{2R}^c)^\top \xi_\ell) &= \beta_\ell(z) \|(\mathcal{J}_{2R}^c)^\top \xi_\ell\|^2 = \beta_\ell(z) \|\xi_\ell\|^2. \end{aligned}$$

Using the orthogonality properties of $\mathcal{P}_{2(\ell-1)}$, the fact that $\xi_\ell, (\mathcal{J}_{2R}^c)^\top \xi_\ell \in \mathcal{V}_{2\ell}$ are ℓ^2 -orthogonal to $\mathcal{V}_{2(\ell-1)}$ by construction, combined with the error criterion of the greedy Algorithm 1, results in

$$\begin{aligned} |\alpha_\ell(z)| &= \frac{|(z, \xi_\ell)|}{\|\xi_\ell\|^2} = \frac{|(z - \mathcal{P}_{2(\ell-1)} z, \xi_\ell)|}{\|\xi_\ell\|^2} \leq \frac{\|z - \mathcal{P}_{2(\ell-1)} z\|}{\|e_\ell - \mathcal{P}_{2(\ell-1)} e_\ell\|} \leq 1, \\ |\beta_\ell(z)| &= \frac{|(z, (\mathcal{J}_{2R}^c)^\top \xi_\ell)|}{\|(\mathcal{J}_{2R}^c)^\top \xi_\ell\|^2} = \frac{|(z - \mathcal{P}_{2(\ell-1)} z, (\mathcal{J}_{2R}^c)^\top \xi_\ell)|}{\|(\mathcal{J}_{2R}^c)^\top \xi_\ell\|^2} \leq \frac{\|z - \mathcal{P}_{2(\ell-1)} z\|}{\|e_\ell - \mathcal{P}_{2(\ell-1)} e_\ell\|} \leq 1. \end{aligned} \tag{A.1}$$

The elements of the orthogonal basis spanning $\mathcal{V}_{2(r+1)}$, selected by the greedy algorithm, can be expanded as

$$\xi_i = \sum_{j=1}^i (\gamma_j^i e_j + \delta_j^i (\mathcal{J}_{2R}^c)^\top e_j), \quad \xi_{r+i} = (\mathcal{J}_{2R}^c)^\top \xi_i,$$

for all $i = 2, \dots, r+1$, where $\gamma_i^i = 1$, $\delta_i^i = 0$ and for $j < i$,

$$\gamma_j^i := \sum_{\ell=j}^{i-1} (-\alpha_\ell(e_i) \gamma_j^\ell + \beta_\ell(e_j) \delta_j^\ell), \quad \delta_j^i := \sum_{\ell=j}^{i-1} (\alpha_\ell(e_i) \delta_j^\ell - \beta_\ell(e_j) \gamma_j^\ell).$$

Using (A.1), each coefficient can be bounded as $|\gamma_j^i| < 3^{i-j-1}$, $|\delta_j^i| < 3^{i-j-1}$ if $j < i$, so that

$$|\gamma_j^i| \leq 3^{i-j}, \quad |\delta_j^i| \leq 3^{i-j}, \quad \forall j \leq i.$$

By definition of the Kolmogorov $2r$ -width, given $\lambda > 1$, there exists a $2r$ -dimensional space \mathcal{W}_{2r} such that the angle between \mathcal{Z}_N^s and \mathcal{W}_{2r} satisfies $\sup_{z \in \mathcal{Z}_N^s} \inf_{w \in \mathcal{W}_{2r}} \|z - w\| \leq \lambda d_{2r}(\mathcal{Z}_N^s)$. Hence, for the elements of any subspace $\mathcal{V}_\ell \subset \mathcal{Z}_N^s$ with $\ell \leq r$, there exist $w_\ell, v_\ell \in \mathcal{W}_{2r}$ such that $\|e_\ell - w_\ell\| \leq \lambda d_{2r}(\mathcal{Z}_N^s)$, and $\|(\mathcal{J}_{2R}^c)^\top e_\ell - v_\ell\| \leq \lambda d_{2r}(\mathcal{Z}_N^s)$. For $i = 1, \dots, r$, we define the vectors

$$\mathcal{W}_{2r} \ni \zeta_i = \sum_{j=1}^i (\gamma_j^i w_j + \delta_j^i v_j), \quad \zeta_{r+i} = \sum_{j=1}^i (-\delta_j^i w_j + \gamma_j^i v_j). \tag{A.2}$$

For $i = 1, \dots, 2r$, they satisfy

$$\|\xi_i - \zeta_i\| \leq \sum_{j=1}^i (|\gamma_j^i| \|e_j - w_j\| + |\delta_j^i| \|(\mathcal{J}_{2R}^c)^\top e_j - v_j\|) \leq \lambda d_{2r}(\mathcal{Z}_N^s) \sum_{j=1}^i 2 \cdot 3^{i-j} < 3^i \lambda d_{2r}(\mathcal{Z}_N^s).$$

Let us consider the elements, defined in (A.2), where we add a further pair $(\zeta_{r+1}, \zeta_{2(r+1)}) \in W_{2r}$, defined such that $w_{r+1}, v_{r+1} \in W_{2r}$ are the vectors for which $\|e_{r+1} - w_{r+1}\| \leq \lambda d_{2r}(\mathcal{Z}_N^s)$, and $\|(\mathcal{J}_{2R}^c)^\top e_{r+1} - v_{r+1}\| \leq \lambda d_{2r}(\mathcal{Z}_N^s)$. Since such a family belongs to the $2r$ -dimensional space W_{2r} by construction, the vectors $\{\zeta_i\}_{i=1}^{2(r+1)}$ cannot be linearly independent: there exist $\{\sigma_i\}_{i=1}^{2(r+1)} \subset \mathbb{R}$ such that $\|\sigma\| = 1$ and $\sum_{i=1}^{2(r+1)} \sigma_i \zeta_i = 0$. Hence,

$$\begin{aligned} \left\| \sum_{i=1}^{r+1} (\sigma_i \xi_i + \sigma_{(r+1)+i} (\mathcal{J}_{2R}^c)^\top \xi_i) \right\| &= \left\| \sum_{i=1}^{2(r+1)} \sigma_i (\xi_i - \zeta_i) \right\| \leq \lambda d_{2r}(\mathcal{Z}_N) \sum_{i=1}^{2(r+1)} |\sigma_i| 3^i \\ &\leq 3^{r+1} \sqrt{2(r+1)} \lambda d_{2r}(\mathcal{Z}_N^s). \end{aligned}$$

Let $1 \leq j \leq 2(r+1)$ be fixed. Define $w_j := \sigma_j^{-1} \sum_{i=1, i \neq j}^{2(r+1)} \sigma_i \xi_i$. Note that $(\xi_j, w_j) = 0$ since $\{\xi_j\}_{j=1}^{2(r+1)}$ is orthogonal, which implies $\|\xi_j + w_j\|^2 \leq \|\xi_j\|^2 + \|w_j\|^2 = \|\xi_j + w_j\|^2$. Furthermore,

$$\|\xi_j + w_j\| \leq \left\| \sigma_j^{-1} \sum_{i=1}^{2(r+1)} \sigma_i (\xi_i - \zeta_i) \right\| \leq |\sigma_j^{-1}| \sum_{i=1}^{2(r+1)} |\sigma_i| \|\xi_i - \zeta_i\| \leq 3^{r+1} \lambda d_{2r}(\mathcal{Z}_N^s) \sqrt{2(r+1)} |\sigma_j^{-1}|.$$

Since the choice of the index j is arbitrary, we select j such that $|\sigma_j| \geq (2(r+1))^{-1/2}$, which is possible by definition of $\{\sigma_i\}_i$. Hence, $\|\xi_j + w_j\| \leq 2 \cdot 3^{r+1} (r+1) \lambda d_{2r}(\mathcal{Z}_N)$. Therefore, the projection error of any $z \in \mathcal{Z}_N^s$ can be bounded as

$$\|z - \mathcal{P}_{2r} z\| \leq \|z - \mathcal{P}_{2(j-1)} z\| \leq \|e_j - \mathcal{P}_{2(j-1)} e_j\| = \|\xi_j\| \leq 2 \cdot 3^{r+1} (r+1) \lambda d_{2r}(\mathcal{Z}_N^s).$$

With an argument analogous to the proof of Proposition 3.12, the conclusion follows from the fact that $d_{2r}(\mathcal{Z}_N^s) \leq d_n(\mathcal{Z}_N)$ since, in each time interval, the subsets $\{\mathcal{N}_j\}_j$ are not affected by the reduction.

References

- [1] R. Abraham and J. E. Marsden. *Foundations of mechanics. Second edition*. Addison-Wesley Publishing Company, Inc., Redwood City, CA., 1987.
- [2] B. M. Afkham and J. S. Hesthaven. “Structure preserving model reduction of parametric Hamiltonian systems.” *SIAM J. Sci. Comput.* 39.6 (2017), A2616–A2644.
- [3] V. I. Arnol’d. “On the topology of three-dimensional steady flows of an ideal fluid.” *J. Appl. Math. Mech.* 30 (1966), pp. 223–226.
- [4] V. I. Arnol’d. *Mathematical methods of classical mechanics*. Second. Vol. 60. Graduate Texts in Mathematics. Springer-Verlag, New York, 1989.
- [5] U. M. Ascher and R. I. McLachlan. “Multisymplectic box schemes and the Korteweg-de Vries equation.” *Appl. Numer. Math.* 48.3-4 (2004), pp. 255–269.
- [6] U. M. Ascher and R. I. McLachlan. “On symplectic and multisymplectic schemes for the KdV equation.” *J. Sci. Comput.* 25.1-2 (2005), pp. 83–104.
- [7] M. Barrault, Y. Maday, N. C. Nguyen, and A. T. Patera. “An ‘empirical interpolation’ method: application to efficient reduced-basis discretization of partial differential equations.” *C. R. Math. Acad. Sci. Paris* 339.9 (2004), pp. 667–672.
- [8] P. Betsch and M. Schiebl. “Energy-momentum-entropy consistent numerical methods for large-strain thermoelasticity relying on the GENERIC formalism.” *International Journal for Numerical Methods in Engineering* 119.12 (2019), pp. 1216–1244.
- [9] P. Binev, A. Cohen, W. Dahmen, R. DeVore, G. Petrova, and P. Wojtaszczyk. “Convergence rates for greedy algorithms in reduced basis methods.” *SIAM J. Math. Anal.* 43.3 (2011), pp. 1457–1472.
- [10] J. H. Brandts. “Matlab code for sorting real Schur forms.” *Numer. Linear Algebra Appl.* 9.3 (2002), pp. 249–261.
- [11] A. Buffa, Y. Maday, A. T. Patera, C. Prud’homme, and G. Turinici. “A priori convergence of the greedy algorithm for the parametrized reduced basis method.” *ESAIM Math. Model. Numer. Anal.* 46.3 (2012), pp. 595–603.
- [12] K. Carlberg, R. Tuminaro, and P. Boggs. “Preserving Lagrangian structure in nonlinear model reduction with application to structural dynamics.” *SIAM J. Sci. Comput.* 37.2 (2015), B153–B184.

- [13] P. Chartier, E. Faou, and A. Murua. “An algebraic approach to invariant preserving integrators: the case of quadratic and Hamiltonian invariants.” *Numer. Math.* 103.4 (2006), pp. 575–590.
- [14] S. Chaturantabut and D. C. Sorensen. “Nonlinear model reduction via discrete empirical interpolation.” *SIAM J. Sci. Comput.* 32.5 (2010), pp. 2737–2764.
- [15] S. Chaturantabut and D. C. Sorensen. “A state space error estimate for POD-DEIM nonlinear model reduction.” *SIAM J. Numer. Anal.* 50.1 (2012), pp. 46–63.
- [16] A. Clebsch. “Ueber die Integration der hydrodynamischen Gleichungen.” *J. Reine Angew. Math.* 56 (1859), pp. 1–10.
- [17] A. Cohen and R. DeVore. “Kolmogorov widths under holomorphic mappings.” *IMA J. Numer. Anal.* 36.1 (2016), pp. 1–12.
- [18] D. Cohen and E. Hairer. “Linear energy-preserving integrators for Poisson systems.” *BIT* 51.1 (2011), pp. 91–101.
- [19] G. Dahlquist. “Stability and error bounds in the numerical integration of ordinary differential equations.” *Kungl. Tekn. Högsk. Handl. Stockholm. No. 130* (1959), p. 87.
- [20] G. Darboux. “Sur le problème de Pfaff.” *Bulletin des Sciences Mathématiques et Astronomiques* 6.1 (1882), pp. 14–36.
- [21] R. A. DeVore. “The Theoretical Foundation of Reduced Basis Methods.” *Model Reduction and Approximation: Theory and Algorithms*. Ed. by P. Benner, M. Ohlberger, A. Cohen, and K. Willcox. Society for Industrial and Applied Mathematics, 2017. Chap. 3, pp. 137–168.
- [22] T. Ergenç and B. Karasözen. “Poisson integrators for Volterra lattice equations.” *Appl. Numer. Math.* 56.6 (2006), pp. 879–887.
- [23] H. Faßbender and K. D. Ikramov. “Some observations on the Youla form and conjugate-normal matrices.” *Linear Algebra Appl.* 422.1 (2007), pp. 29–38.
- [24] L. Giraud, J. Langou, M. Rozložník, and J. van den Eshof. “Rounding error analysis of the classical Gram-Schmidt orthogonalization process.” *Numer. Math.* 101.1 (2005), pp. 87–100.
- [25] V. Grimm and G. R. W. Quispel. “Geometric integration methods that preserve Lyapunov functions.” *BIT* 45.4 (2005), pp. 709–723.
- [26] T. H. Gronwall. “Note on the derivatives with respect to a parameter of the solutions of a system of differential equations.” *Ann. of Math. (2)* 20.4 (1919), pp. 292–296.
- [27] E. Hairer, C. Lubich, and G. Wanner. *Geometric numerical integration*. Second. Vol. 31. Springer Series in Computational Mathematics. Springer-Verlag, Berlin, 2006.
- [28] A. Kolmogorov. “Über die beste Annäherung von Funktionen einer gegebenen Funktionenklasse.” *Ann. of Math. (2)* 37.1 (1936), pp. 107–110.
- [29] M. Kraus, K. Kormann, P. J. Morrison, and E. Sonnendrücker. “GEMPIC: geometric electromagnetic particle-in-cell methods.” *Journal of Plasma Physics* 83.4 (2017), p. 905830401.
- [30] S. Lall, P. Krysl, and J. E. Marsden. “Structure-preserving model reduction for mechanical systems.” *Phys. D* 184.1-4 (2003), pp. 304–318.
- [31] S. Lie. “Theorie der Transformationsgruppen I.” *Math. Ann.* 16.4 (1880), pp. 441–528.
- [32] R. G. Littlejohn. “A guiding center Hamiltonian: A new approach.” *Journal of Mathematical Physics* 20.12 (1979), pp. 2445–2458.
- [33] J. E. Marsden. “Darboux’s theorem fails for weak symplectic forms.” *Proc. Amer. Math. Soc.* 32 (1972), pp. 590–592.
- [34] J. E. Marsden and T. S. Ratiu. *Introduction to mechanics and symmetry*. Second. Vol. 17. Texts in Applied Mathematics. Springer-Verlag, New York, 1999.
- [35] J. E. Marsden and A. Weinstein. “Coadjoint orbits, vortices, and Clebsch variables for incompressible fluids.” *Phys. D* 7.1-3 (1983), pp. 305–323.
- [36] R. I. McLachlan, G. R. W. Quispel, and N. Robidoux. “Geometric integration using discrete gradients.” *R. Soc. Lond. Philos. Trans. Ser. A Math. Phys. Eng. Sci.* 357.1754 (1999), pp. 1021–1045.
- [37] P. J. Morrison and J. Vanneste. “Weakly nonlinear dynamics in noncanonical Hamiltonian systems with applications to fluids and plasmas.” *Ann. Physics* 368 (2016), pp. 117–147.
- [38] A. Natale and C. J. Cotter. “A variational $H(\text{div})$ finite-element discretization approach for perfect incompressible fluids.” *IMA J. Numer. Anal.* 38.3 (2018), pp. 1388–1419.
- [39] P. J. Olver. “Darboux’s theorem for Hamiltonian differential operators.” *J. Differential Equations* 71.1 (1988), pp. 10–33.
- [40] L. Peng and K. Mohseni. “Symplectic model reduction of Hamiltonian systems.” *SIAM J. Sci. Comput.* 38.1 (2016), A1–A27.
- [41] A. Salam. “On theoretical and numerical aspects of symplectic Gram-Schmidt-like algorithms.” *Numer. Algorithms* 39.4 (2005), pp. 437–462.
- [42] A. Weinstein. “Symplectic manifolds and their Lagrangian submanifolds.” *Advances in Math.* 6 (1971), pp. 329–346.
- [43] A. Weinstein. “The local structure of Poisson manifolds.” *J. Differential Geom.* 18.3 (1983), pp. 523–557.
- [44] D. Wirtz, D. C. Sorensen, and B. Haasdonk. “A posteriori error estimation for DEIM reduced nonlinear dynamical systems.” *SIAM J. Sci. Comput.* 36.2 (2014), A311–A338.
- [45] J. Yan and C.-W. Shu. “A local discontinuous Galerkin method for KdV type equations.” *SIAM J. Numer. Anal.* 40.2 (2002), pp. 769–791.
- [46] D. C. Youla. “A normal form for a matrix under the unitary congruence group.” *Canad. J. Math.* 13 (1961), pp. 694–704.